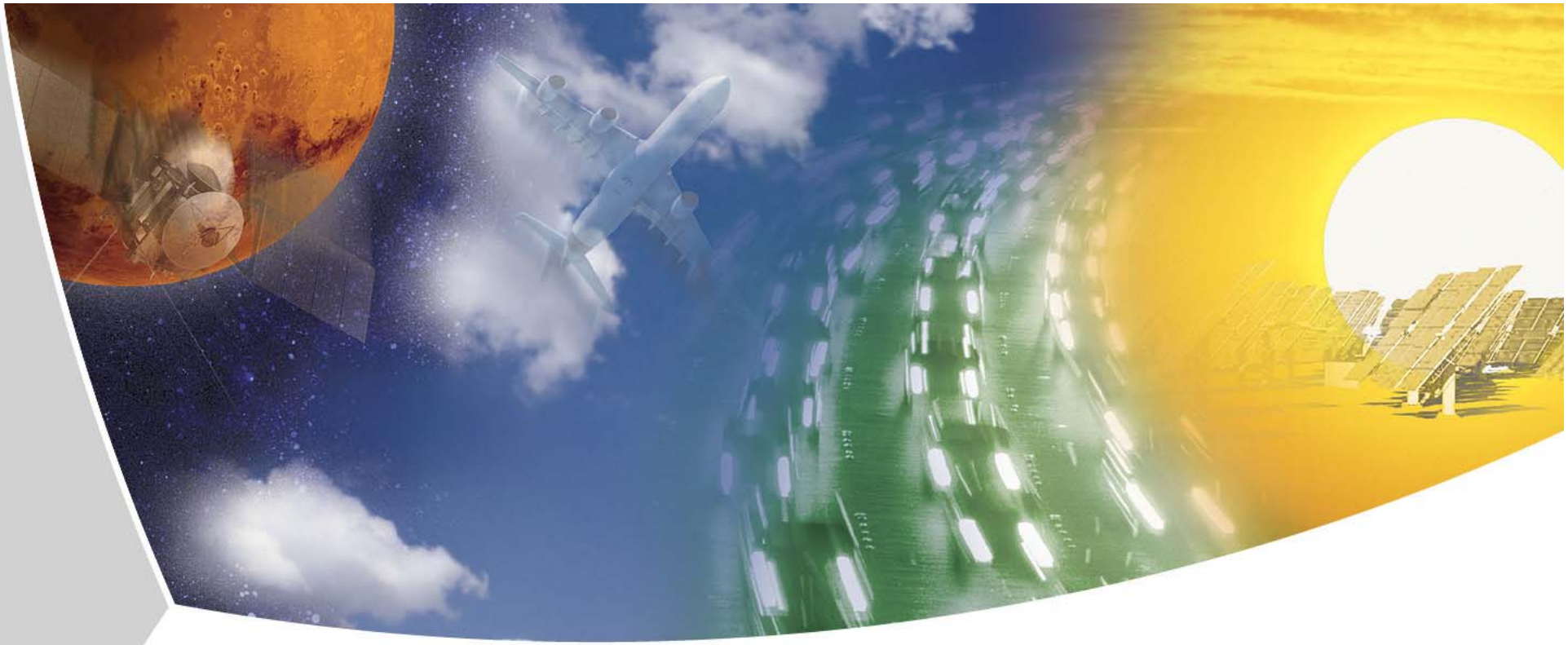

Analysis of coherent terahertz synchrotron radiation with a superconducting hot electron bolometer

H.-W. Hübers

Deutsches Zentrum für Luft- und Raumfahrt

Institut für Planetenforschung

Rutherfordstr. 2, 12489 Berlin

Outline

- Coherent synchrotron radiation at THz frequencies
- Superconducting hot electron bolometer (HEB)
- Single pulse detection with HEB
- Outlook

BESSY II

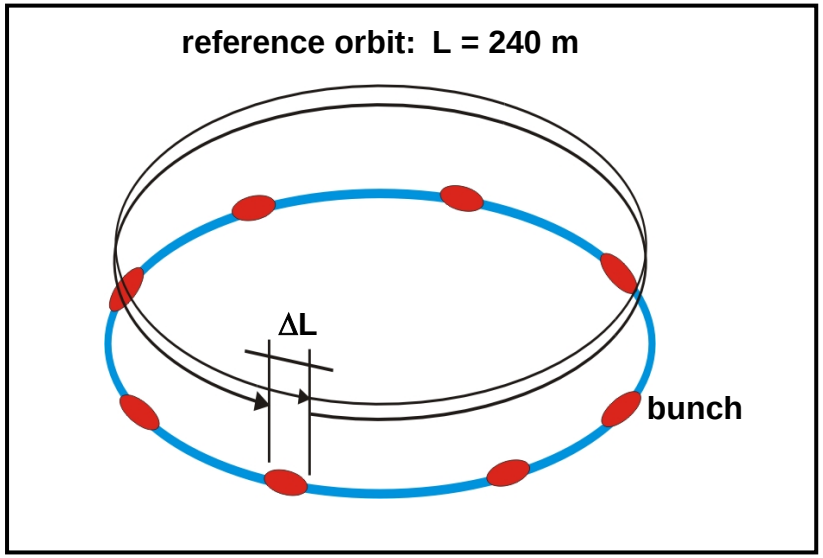

Revolution:
- 1.25 MHz, 0.8 µs, 240 m
- InSb hot electron bolometer ($\tau \approx 1$ µs)

Bunch separation:
- max. 400 bunches
- 500 MHz, 2 ns, 60 cm
- superconducting hot electron bolometer

Bunch length
- >35 ps, >5 mm (normal user optics)
- <7 ps, <1mm (low alpha optics)
- autocorrelation

Coherent THz Radiation from a Synchrotron

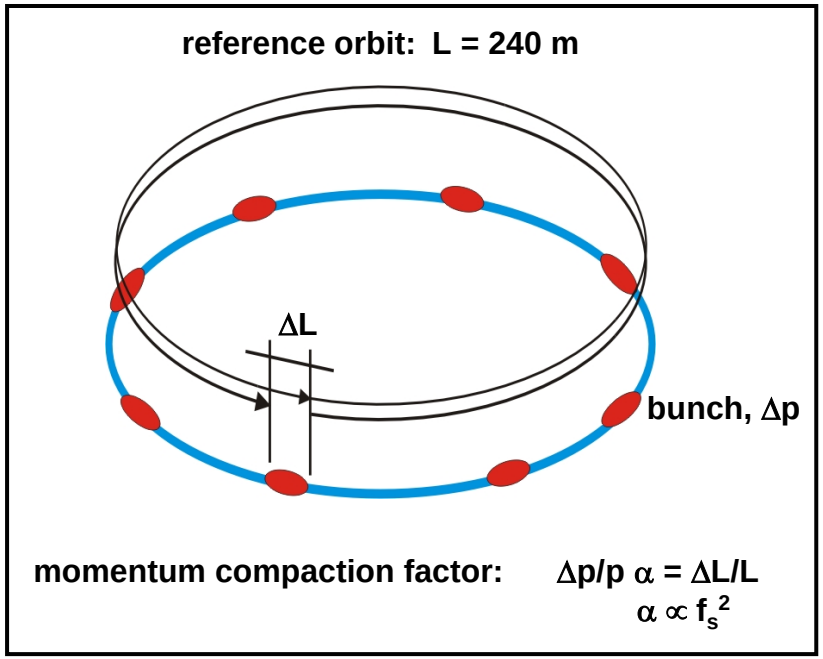

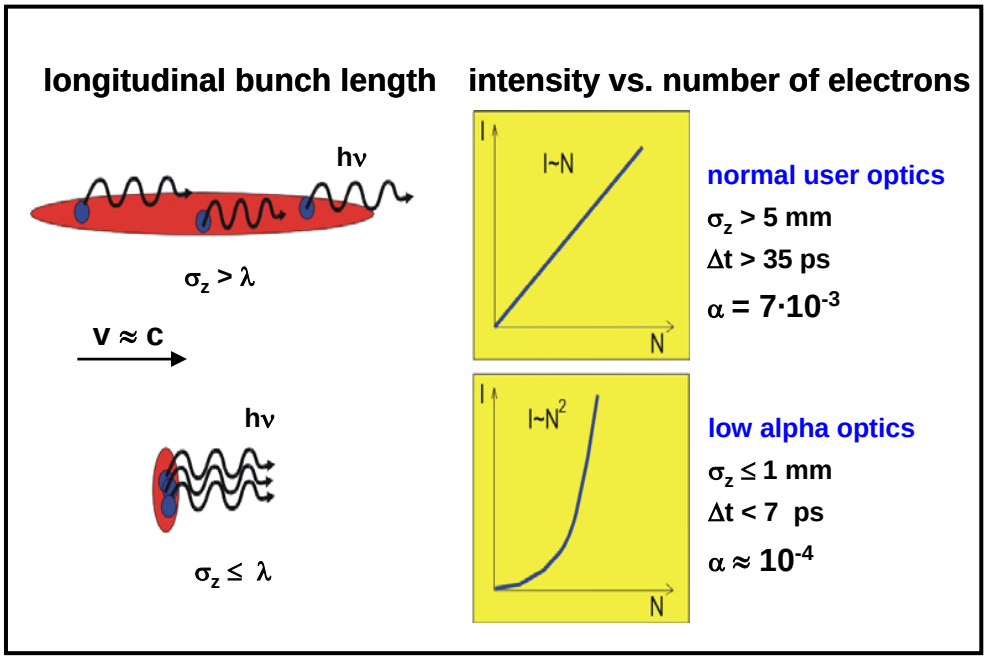

Dedicated machine mode:"low α" optics

- Bunch shortening down to and below the mm-range
- Emission in the THz range is drastically enhanced

$P = N P_1 (1 + N f_\lambda)$

P_1: power from a single electron

N: number of electrons

$f_\lambda = \exp[-(2\pi\sigma/\lambda)^2]$ (form factor)

σ : rms bunch length

Synchrotron Spectrum

N-times higher intensity (Gaussian bunch assumed)

Cut-off due to shielding effects

Powerful source emitting in the THz and sub-THz range

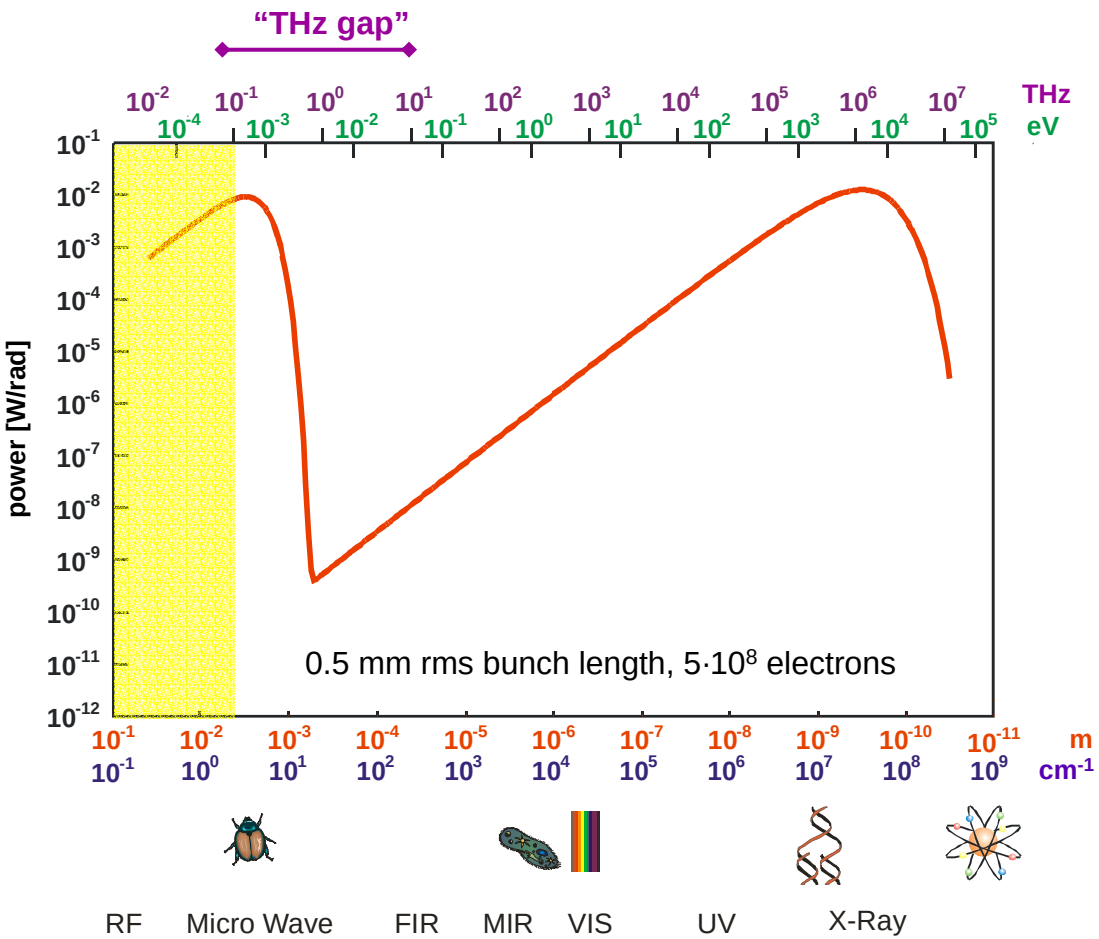

Incoherent vs. Coherent SR

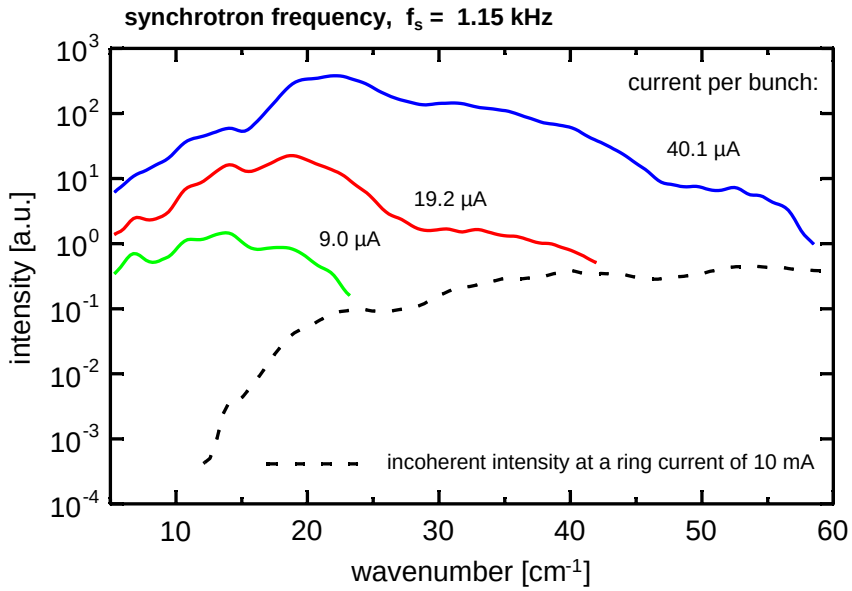

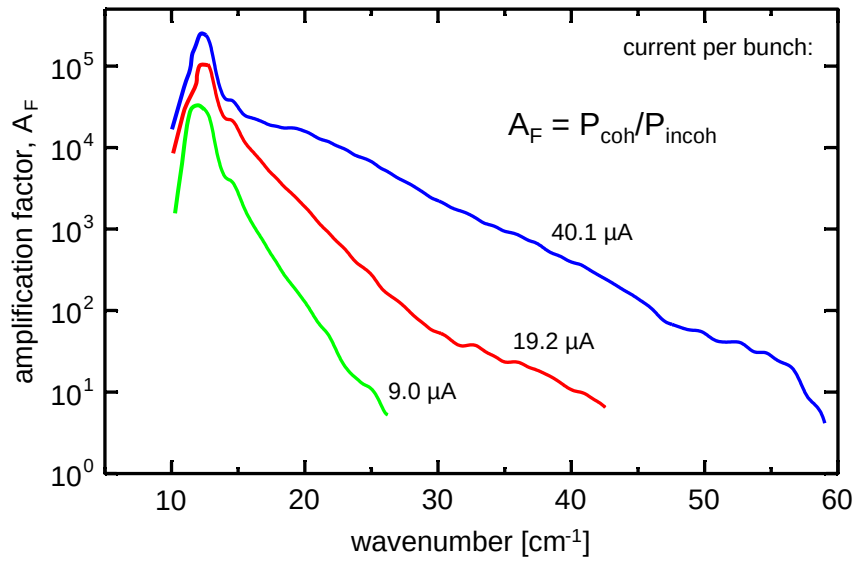

- Intensity extends to higher wavenumbers than expected for Gaussian bunch shape.

- Power increase of up to 100000 compared to the incoherent SR.

M. Abo-Bakr et al., Phys. Rev. Lett. **90**, 094801 (2003)

Applications of CSR

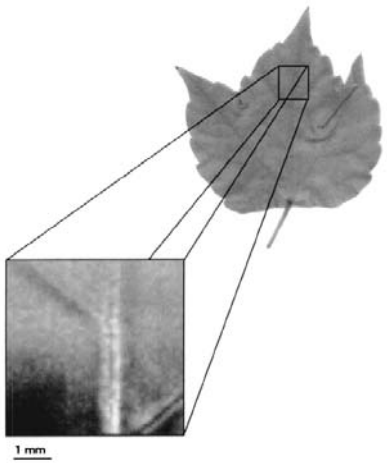

FIG. 4. Near-field THz image of a section of a *parthenocissus* leaf. Note

U. Schade et al., APL **84**, 1422 (2004)

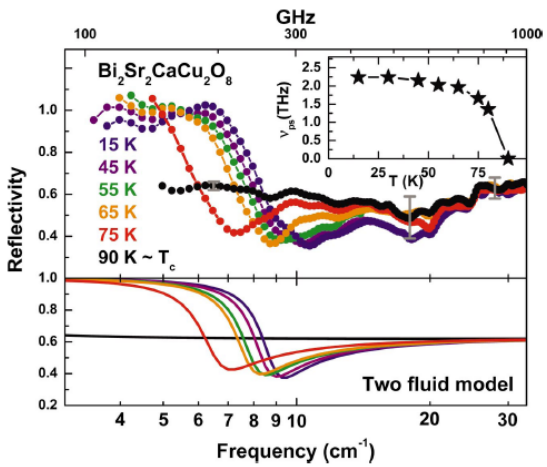

FIG. 2. (Color) Measured *c*-axis polarized near-normal reflectivity of $Bi_2Sr_2CaCu_2O_8$ (upper panel) for various representative temperatures at or below the superconducting transition temperature, T_c. A resonance that shifts with temperature and disappears above T_c is clearly observed. The lower panel shows the calculated reflectivity of a superconductor with a shifting Josephson plasma resonance. The inset of the top panel shows the temperature dependence of the unscreened superfluid plasma frequency as determined from fits to the data.

E.J. Singley et al., PRB **69**, 092512 (2004)

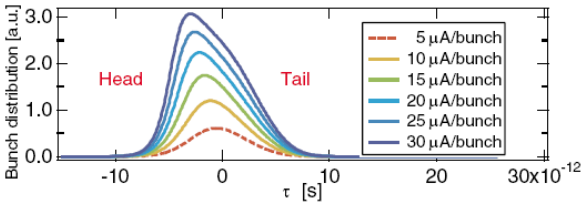

FIG. 1 (color online). Calculated equilibrium longitudinal distribution for different currents per bunch using the shielded SR wake. BESSY II case with a natural bunch length of 2.5 ps.

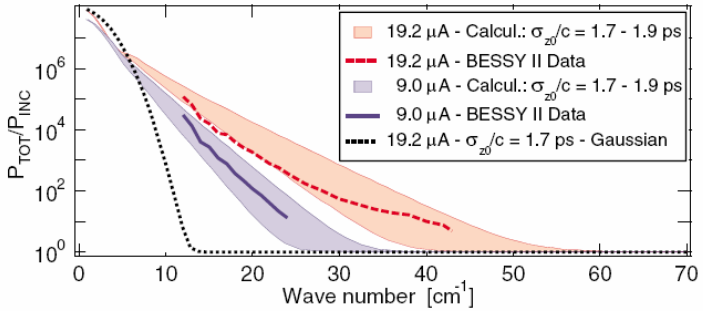

FIG. 2 (color online). CSR gain as a function of the wave number $1/\lambda$. The BESSY II data for two different currents per bunch are compared with the shielded SR calculation and with the curve for a Gaussian distribution of the same length.

F. Sannibale et al., PRL **93**, 094801 (2004)

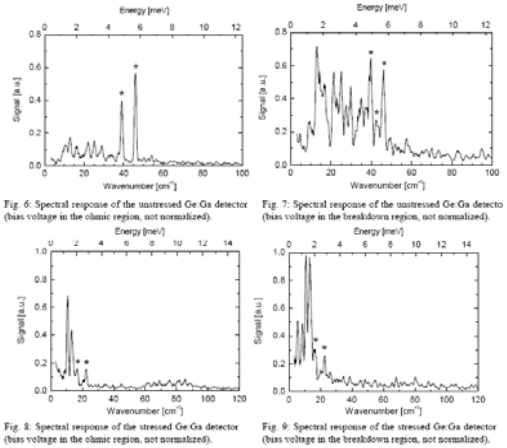

Fig. 6: Spectral response of the unstressed Ge:Ga detector (bias voltage in the ohmic region, not normalized).

Fig. 7: Spectral response of the unstressed Ge:Ga detecto (bias voltage in the breakdown region, not normalized).

Fig. 8: Spectral response of the stressed Ge:Ga detector (bias voltage in the ohmic region, not normalized).

Fig. 9: Spectral response of the stressed Ge:Ga detector (bias voltage in the breakdown region, not normalized).

H.-W. Hübers et al., SPIE **6275**, 627505 (2006)

Bolometer

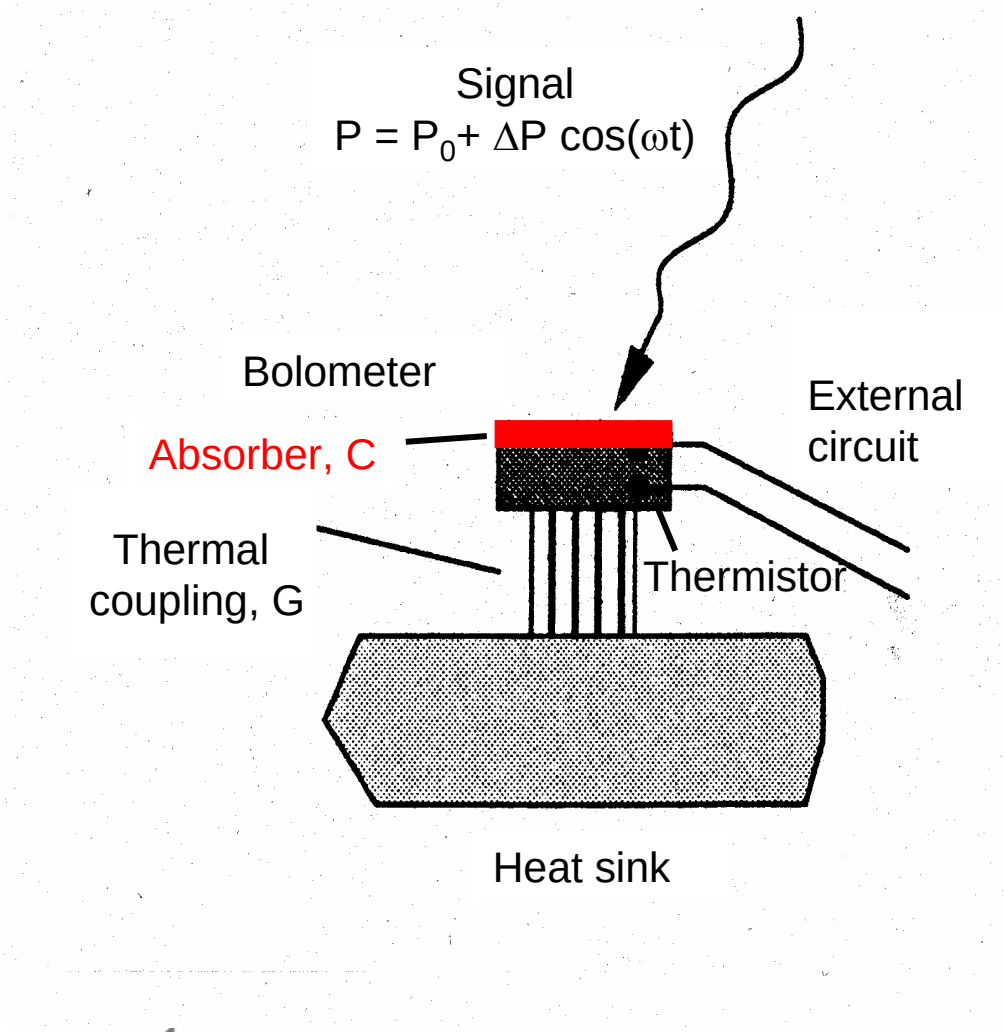

Heat transfer:

$$C \frac{dT}{dt} = P(t) - G\,(T-T_0)$$

C: heat capacity
G: heat conductivity

Temperature modulation:

$$\Delta T = \frac{\Delta P}{G\sqrt{1+\omega^2(C/G)^2}}$$

Responsivity:

$$R(\omega) = \frac{\Delta V}{\Delta P} \propto \frac{1}{G\sqrt{1+\omega^2(C/G)^2}}$$

$$\omega \ll 1/\tau : \quad R(\omega) \propto \frac{1}{G}$$

$$\omega \gg 1/\tau : \quad R(\omega) \propto \frac{1}{\omega C}$$

$\tau = C/G$: bolometer time constant

Superconducting Nanobridge

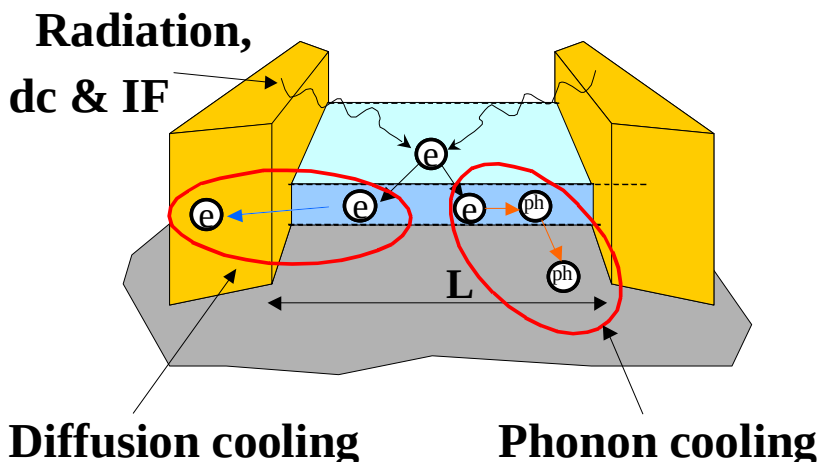

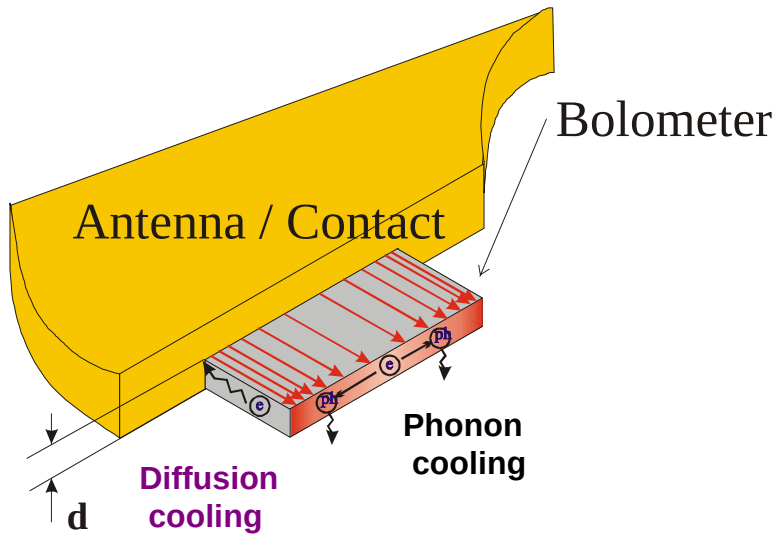

Dimensions:

L: 0.2 - 1.0 µm

w: 1 - 4 µm

d: 3.5 nm

Superconducting Hot-Electron Bolometer

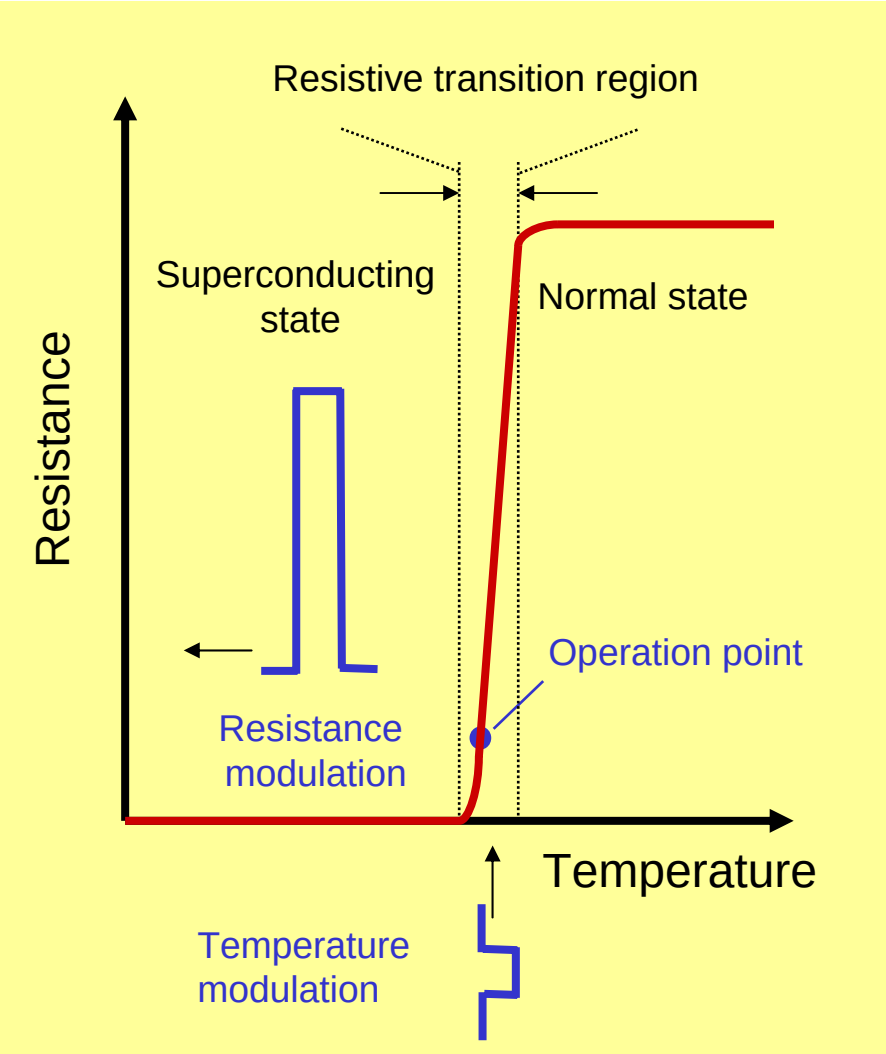

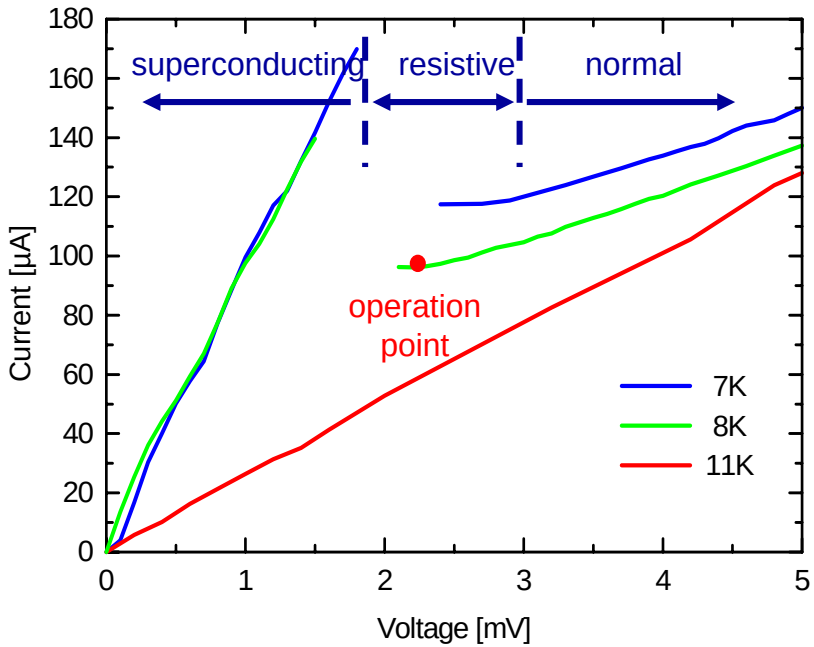

Response Time

Time constants:

$\tau \approx \tau_{e\text{-}ph} + c_{ph}/c_e\, \tau_{esc}$

$\tau_{e\text{-}ph} \approx 10$ ps for NbN ($T_c = 9$ K)

$\tau_{esc} = 4d/\alpha u \approx 38$ ps ($d = 3.5$ nm)

Fast device:

- material with small $\tau_{e\text{-}ph}$, large u
- thin films, small d
- large phonon transmissivity α

Hot Spot Model

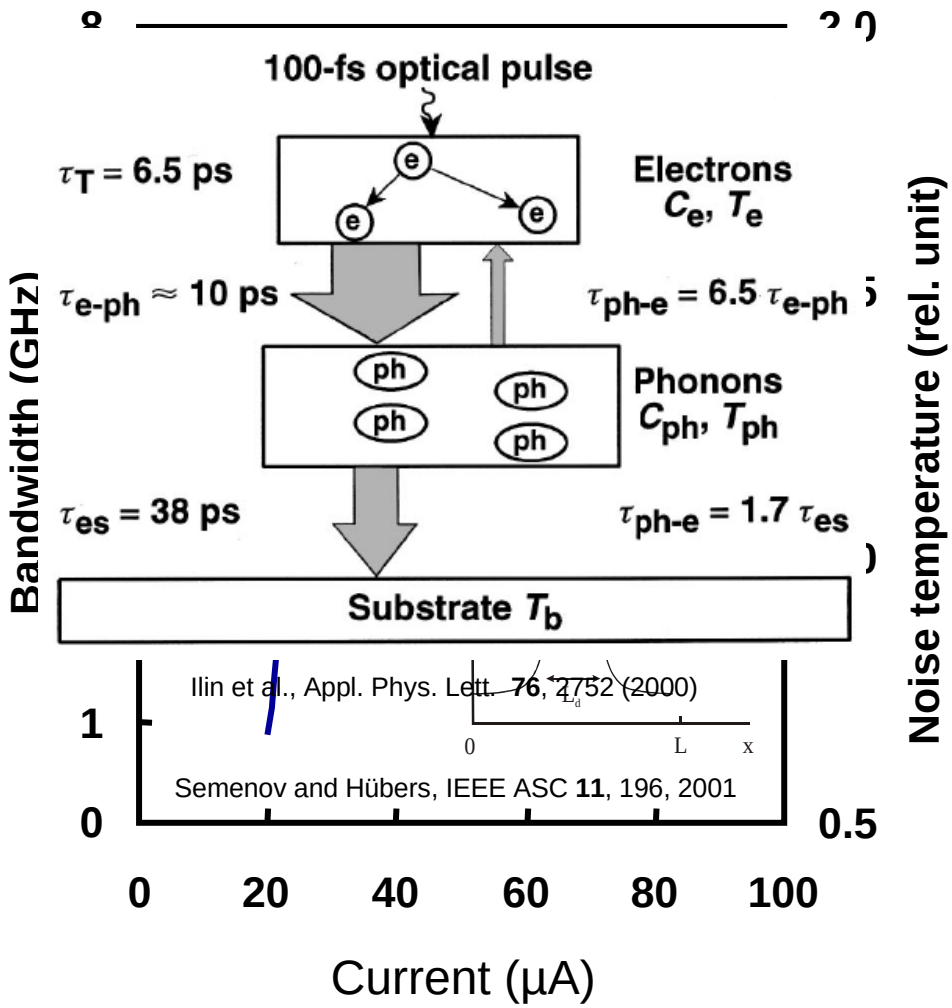

Velocity of domain walls controls the bandwidth.

Measurements of time constants

- electro-optic sampling
- λ = 386 nm
- analysis with 2T model

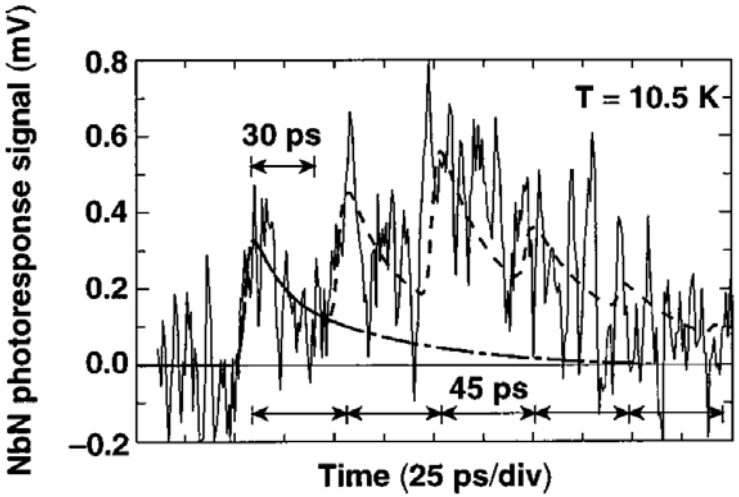

FIG. 2. Time-resolved experimental (solid line) and simulated (dotted and dotted–dashed lines) responses of a 3.5-nm-thick NbN HEP to a 100 fs excitation pulse. Ambient temperature was 10.5 K.

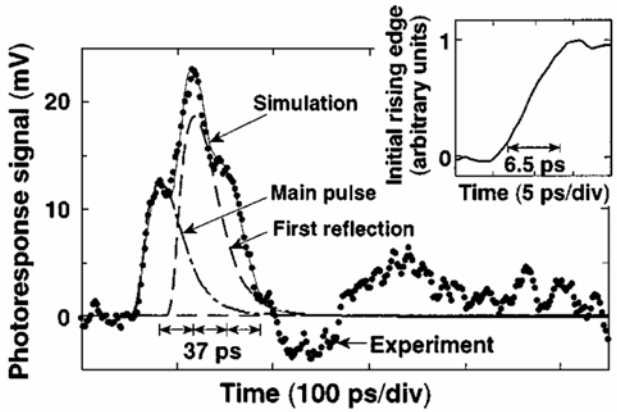

FIG. 1. Experimental (dots) and simulated (solid, dotted, and dotted–dashed lines) responses of a 3.5-nm-thick NbN HEP to a 100 fs excitation pulse. The main plot time resolution is 25 ps; the time-resolved rising part of the signal is shown in inset. Ambient temperature was 2.15 K.

K. Ilin et al., Appl. Phys. Lett. **76**, 2752 (2000)

Design

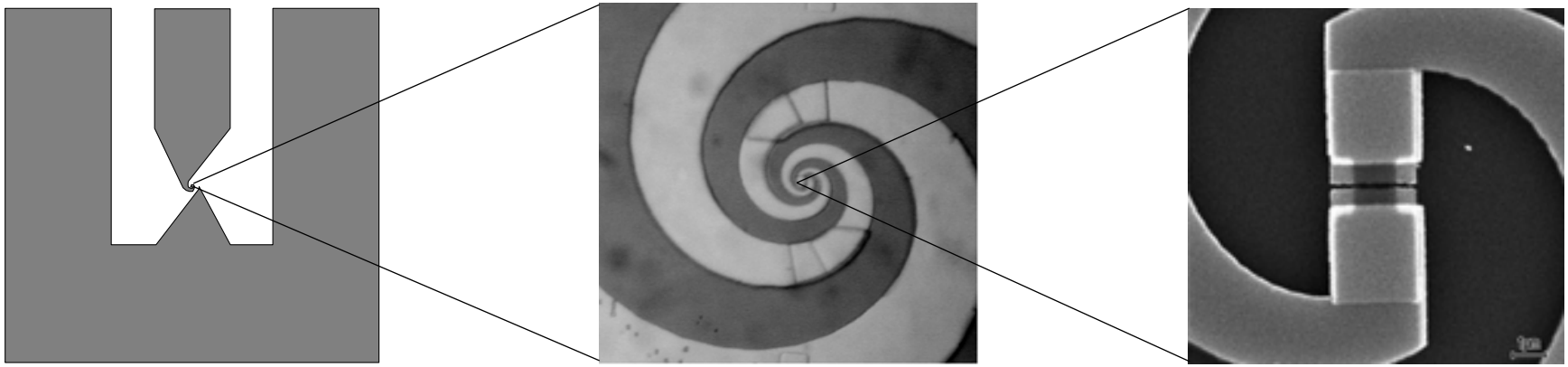

- NbN film: 3.5 nm thick (dc reactive magnetron sputtering)
- Transition temperature: 9 K, width: ≈ 0.5 K
- Si substrate: > 10 kΩ cm
- Two arm log-spiral antenna terminated by 50 Ω coplanar line

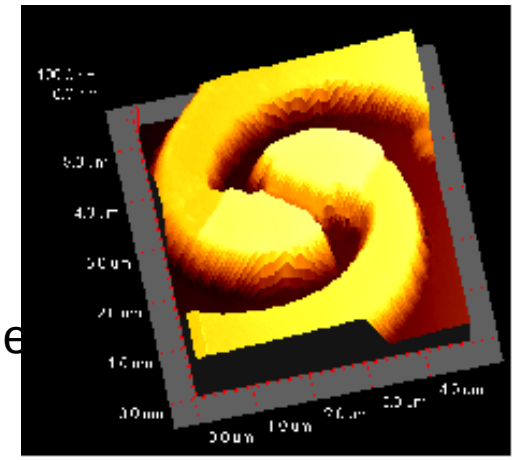

J. Appl. Phys. 88, 6758 (2000)

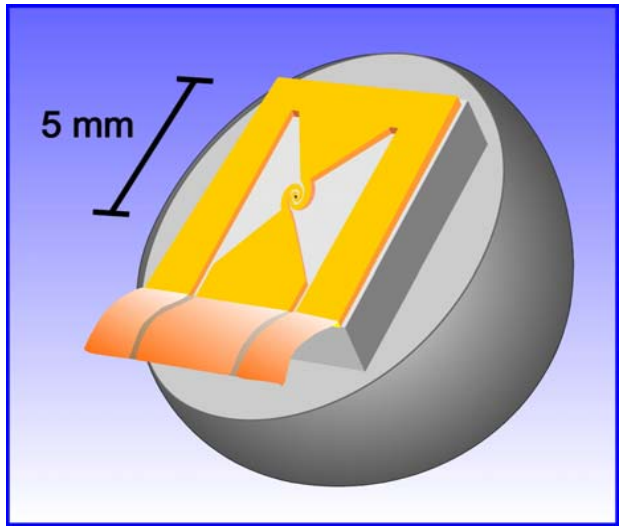

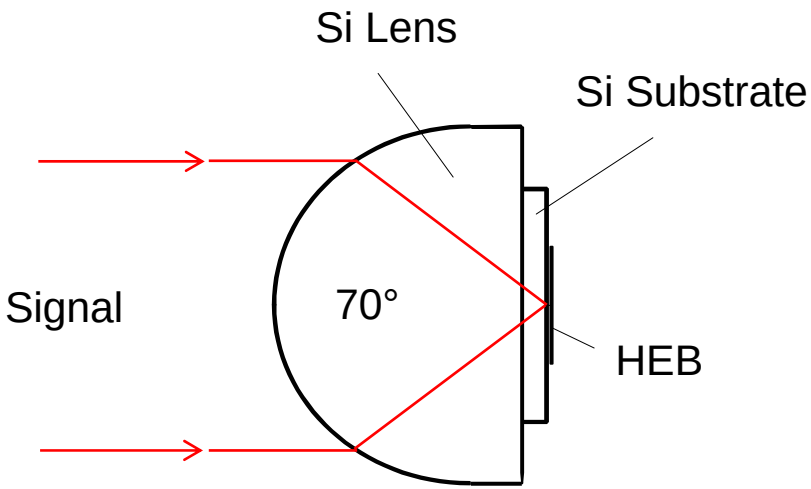

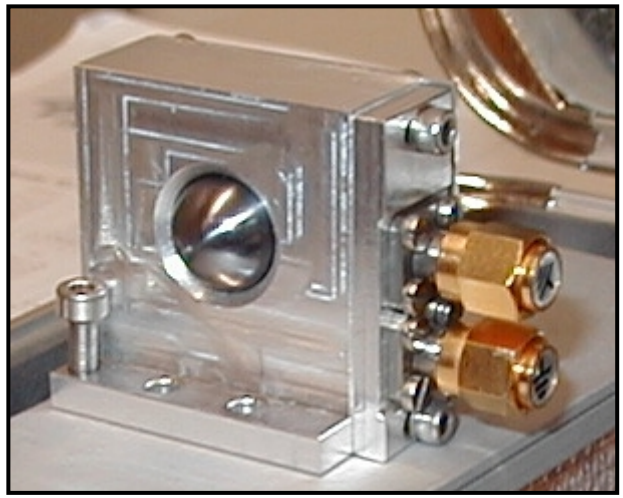

6 or 12 mm diameter extended hemispherical Si lens with Parylene AR coating.

Antenna Pattern

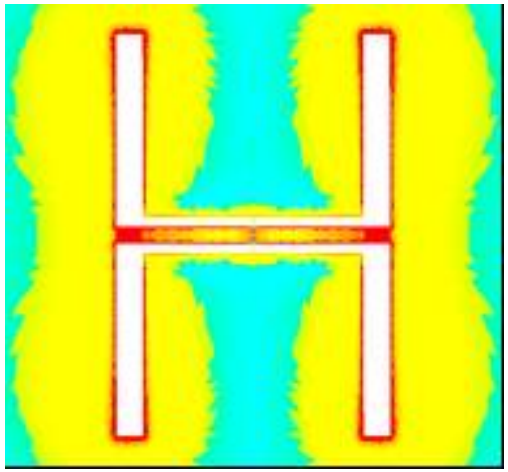

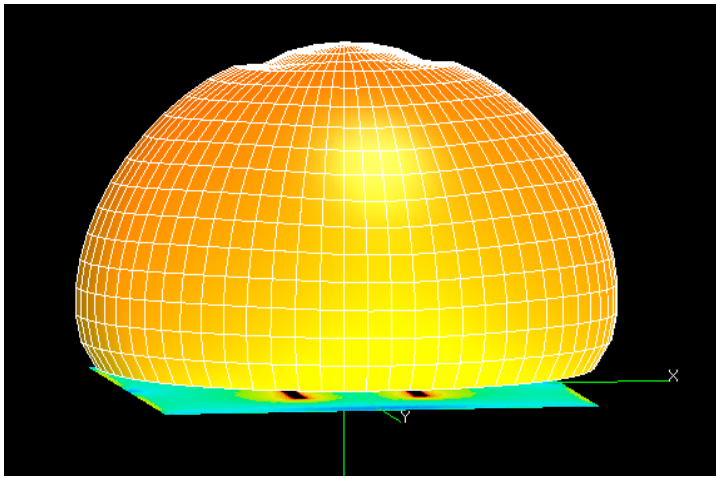

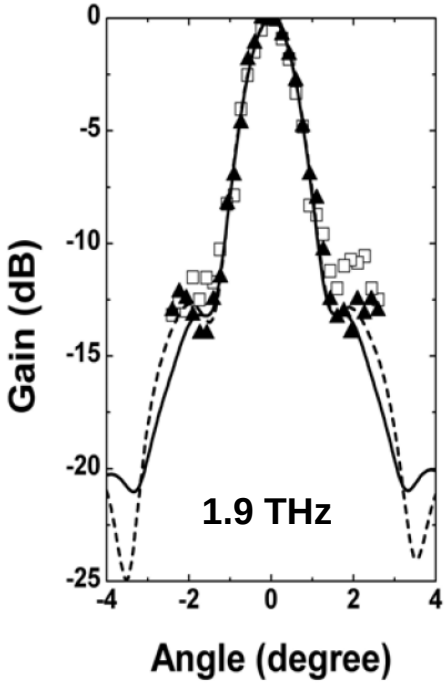

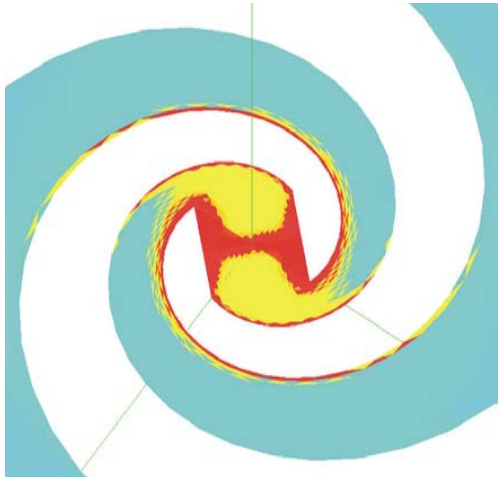

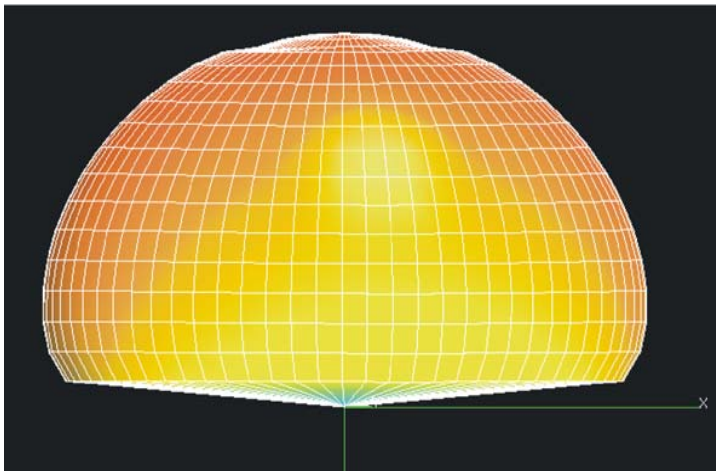

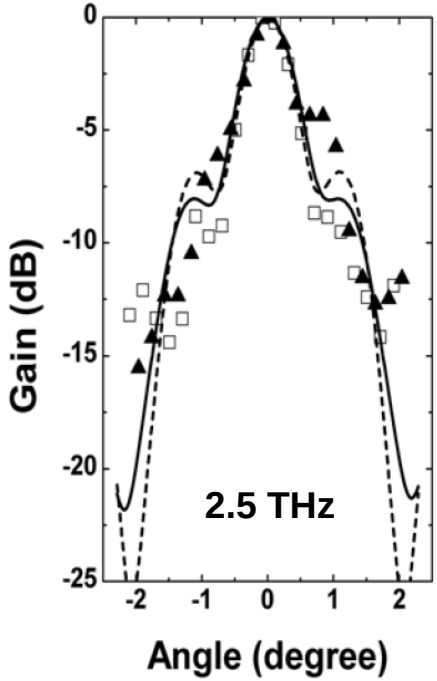

A. Semenov et al., accepted IEEE MTT 2006

Antenna Pattern

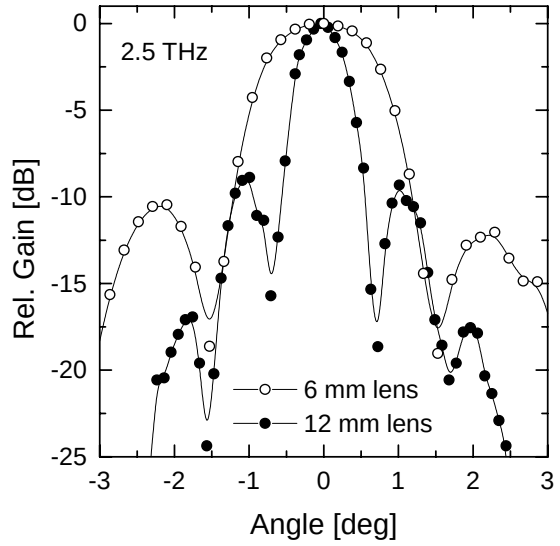

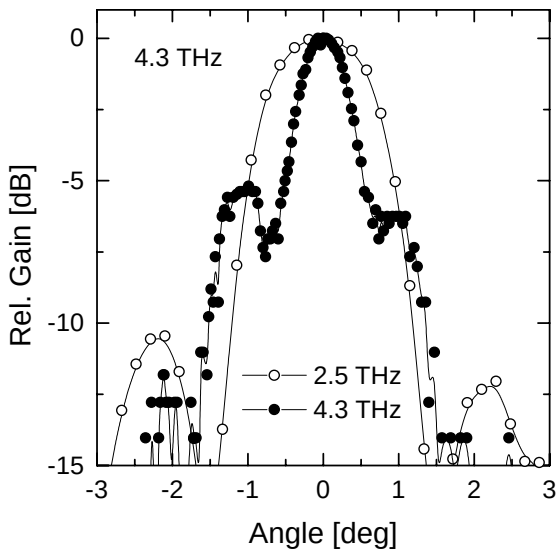

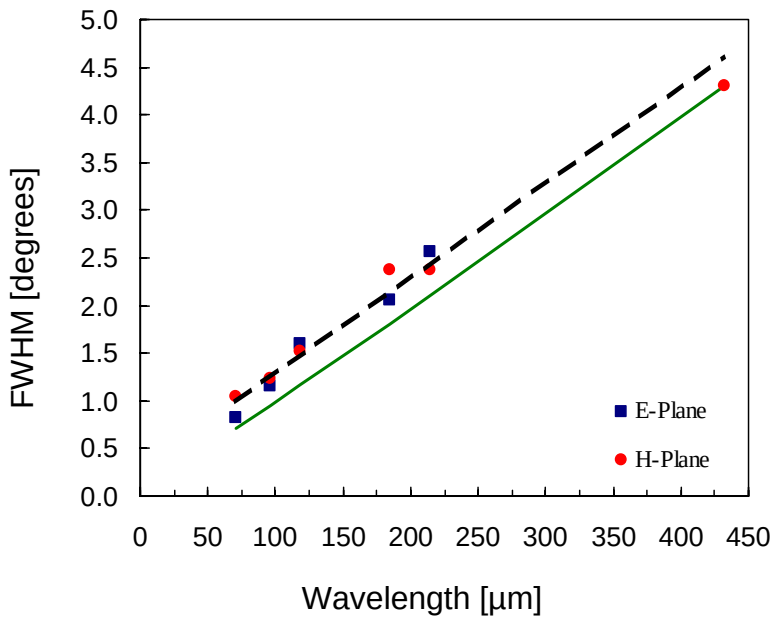

Spectral Response

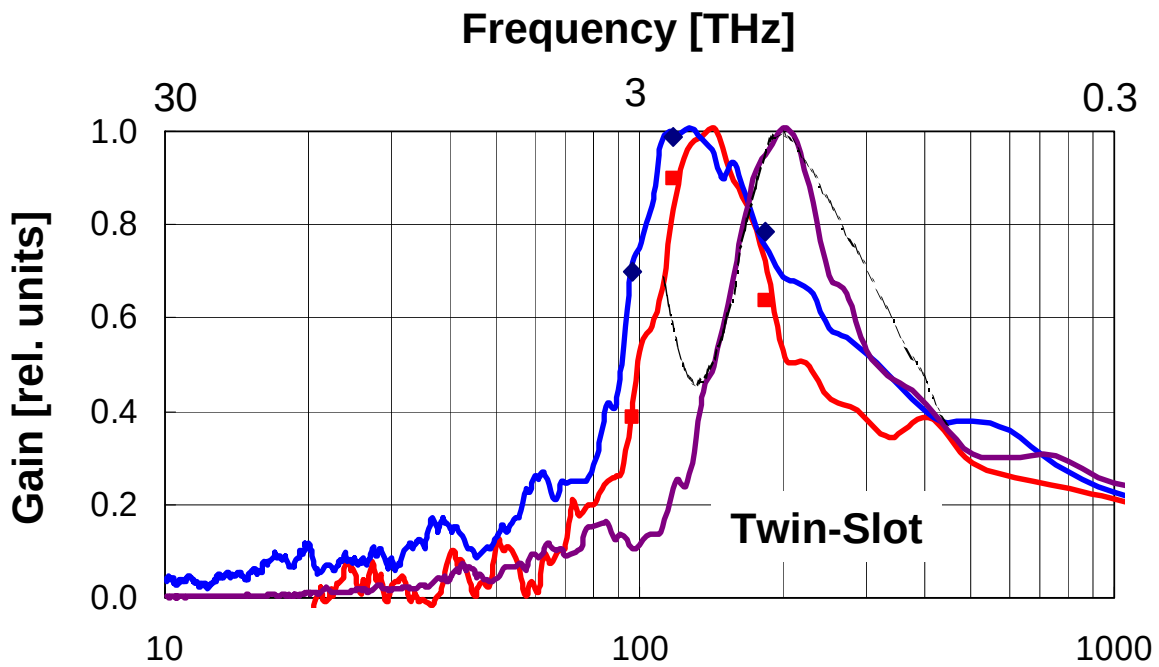

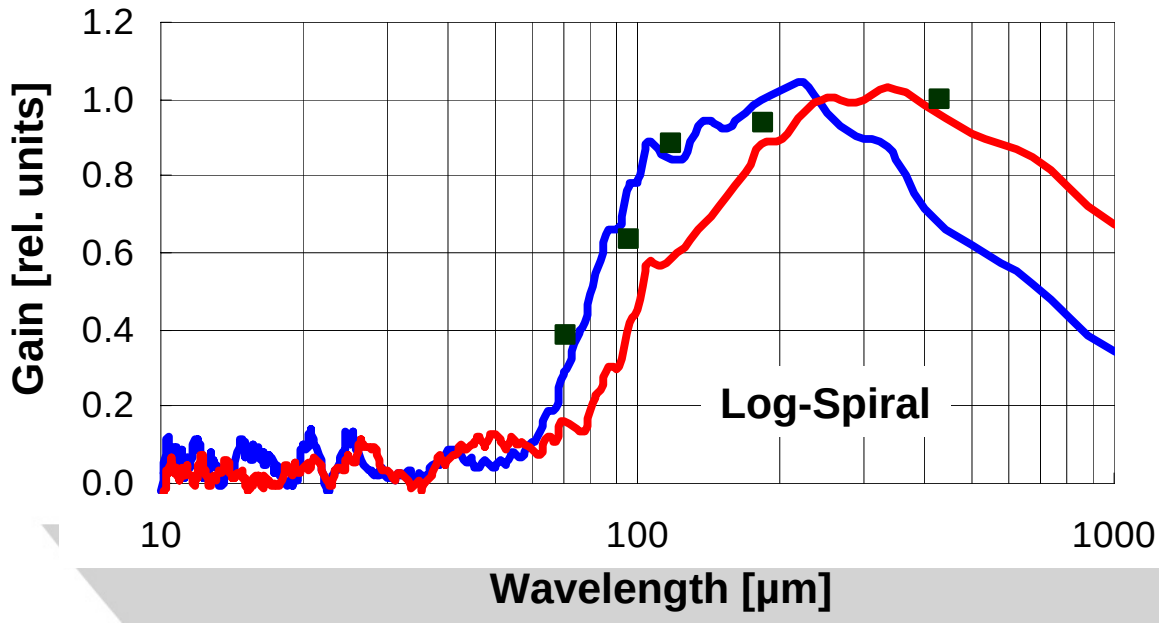

Spectroscopy: Experimental Setup

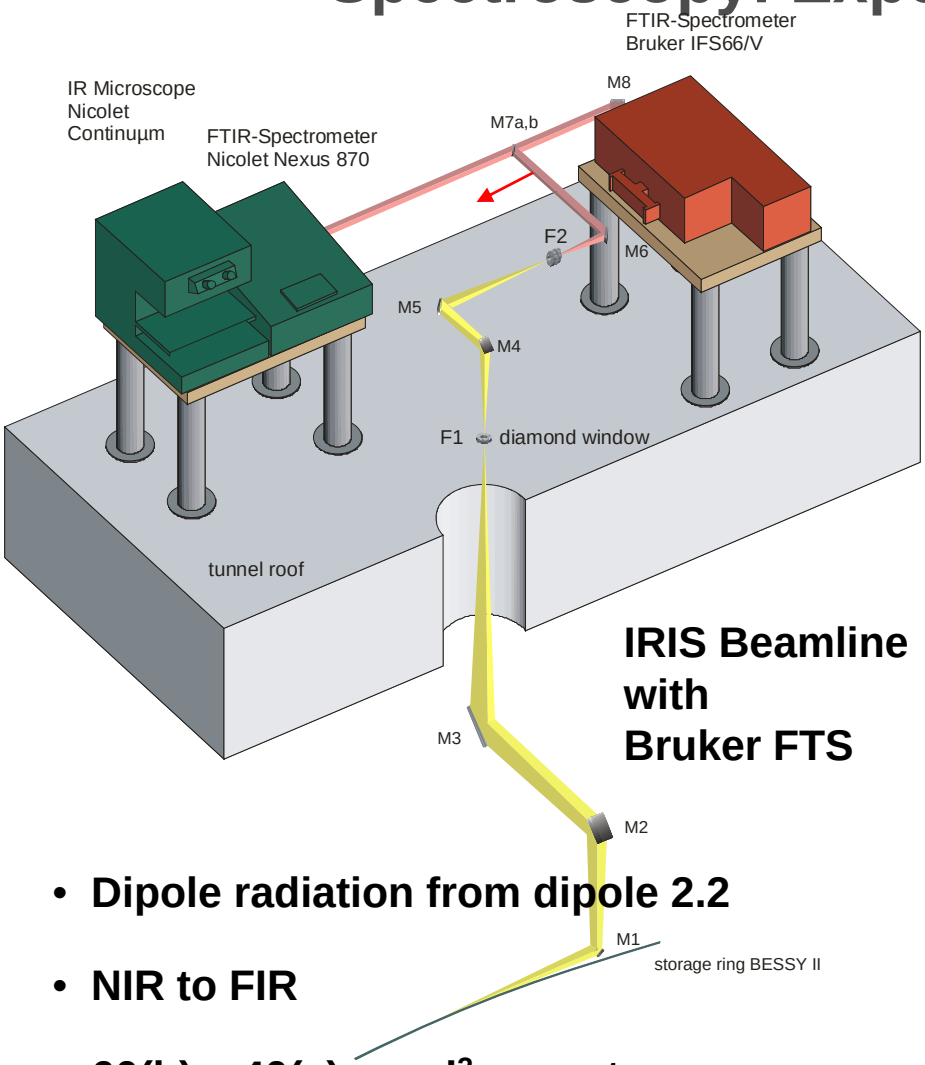

IRIS Beamline with Bruker FTS

- **Dipole radiation from dipole 2.2**
- **NIR to FIR**
- **60(h) x 40(v) mrad^2 acceptance**

Martin-Puplett Spectrometer at IRIS Beamline

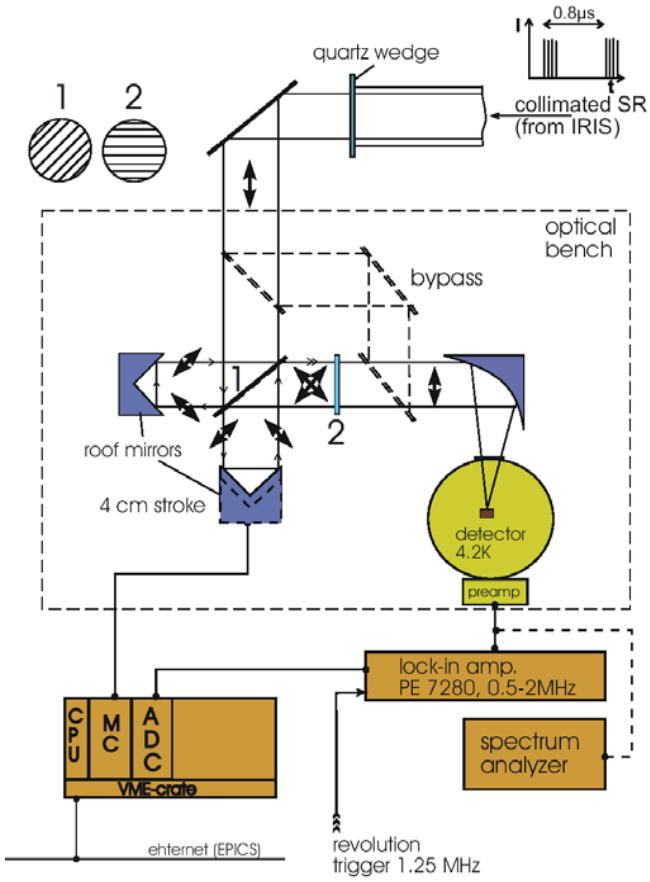

Experimental Setup

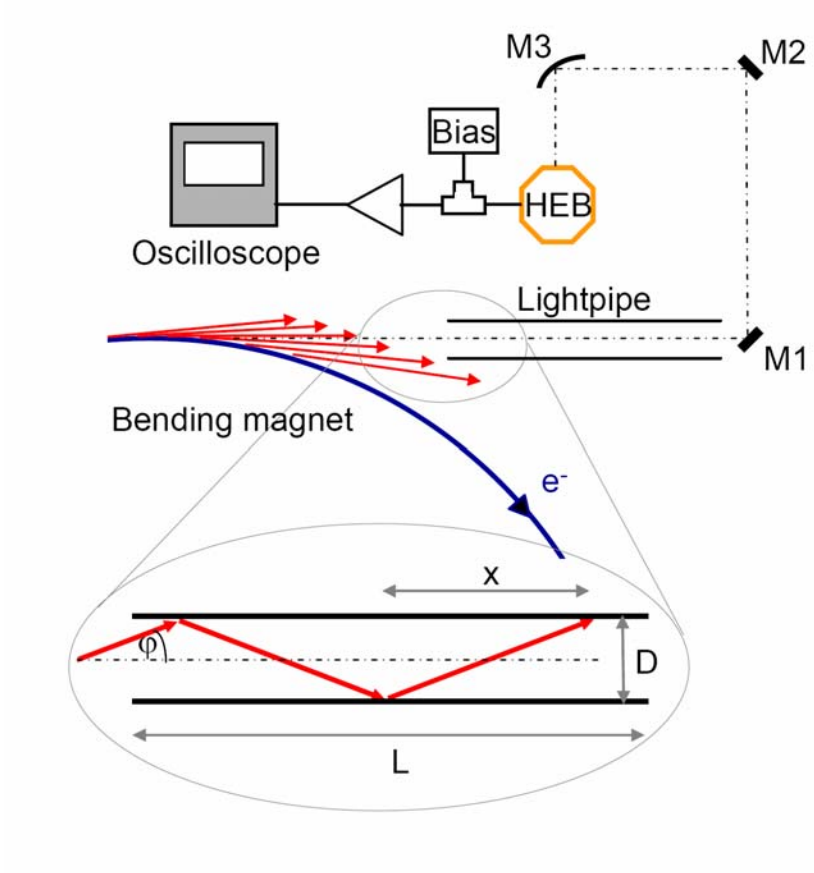

- about 9 m from source point to detector
- Bias-T: 0.1 -18 GHz
- Amplifier: 0.1-12 GHz
- Sampling oscilloscope: 50 GHz

Measurement with InSb Detector

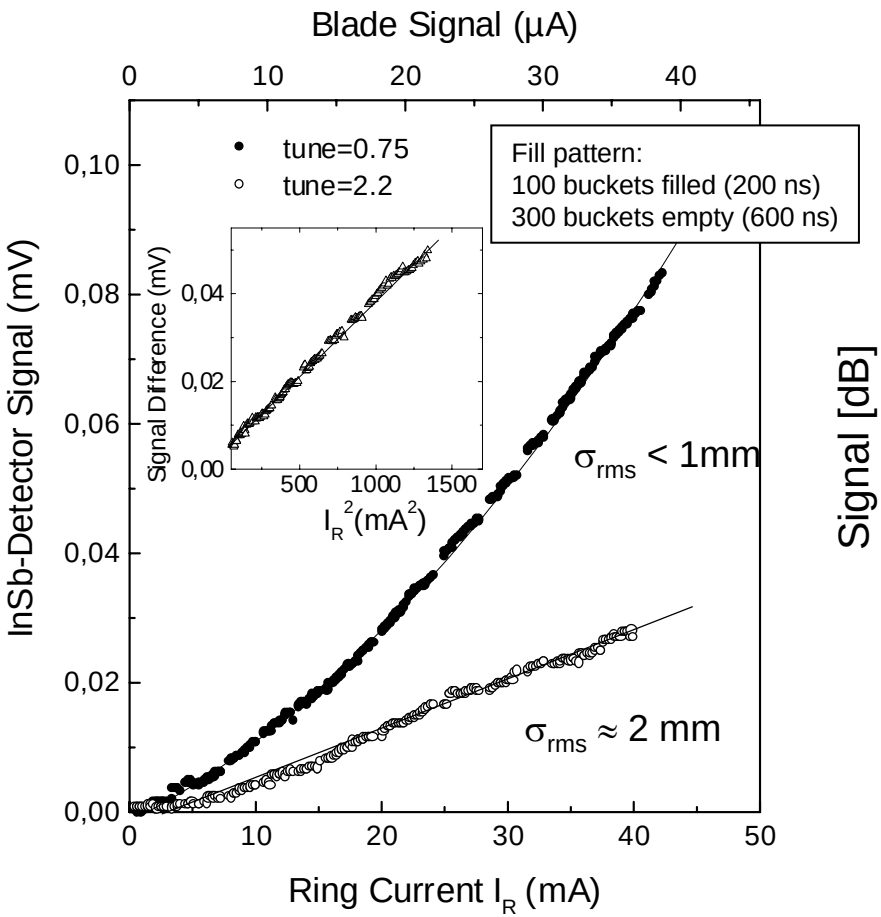

Single bunch CSR intensity and threshold at 1.25 MHz

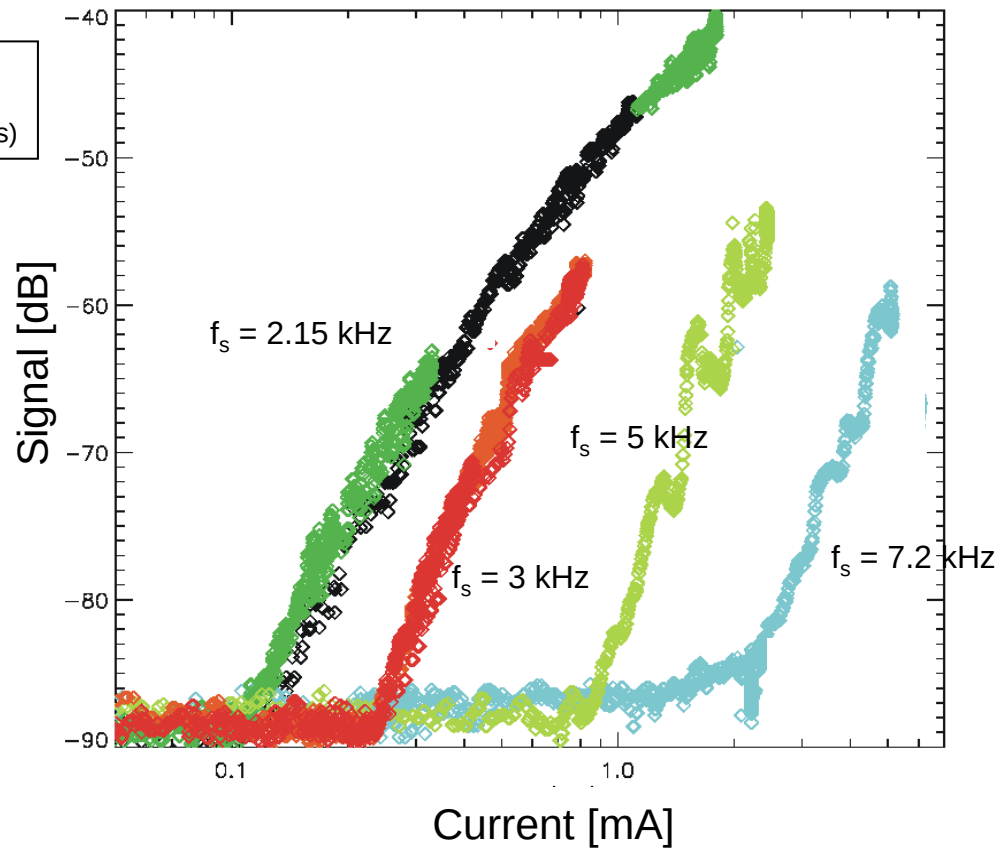

InSb detector ($\tau_{rise} \approx$ 200 ns, $\tau_{decay} \approx$ 400 ns)

M. Abo-Bakr et al., Phys. Rev. Lett. **88**, 25481, 2002

Beam Filling

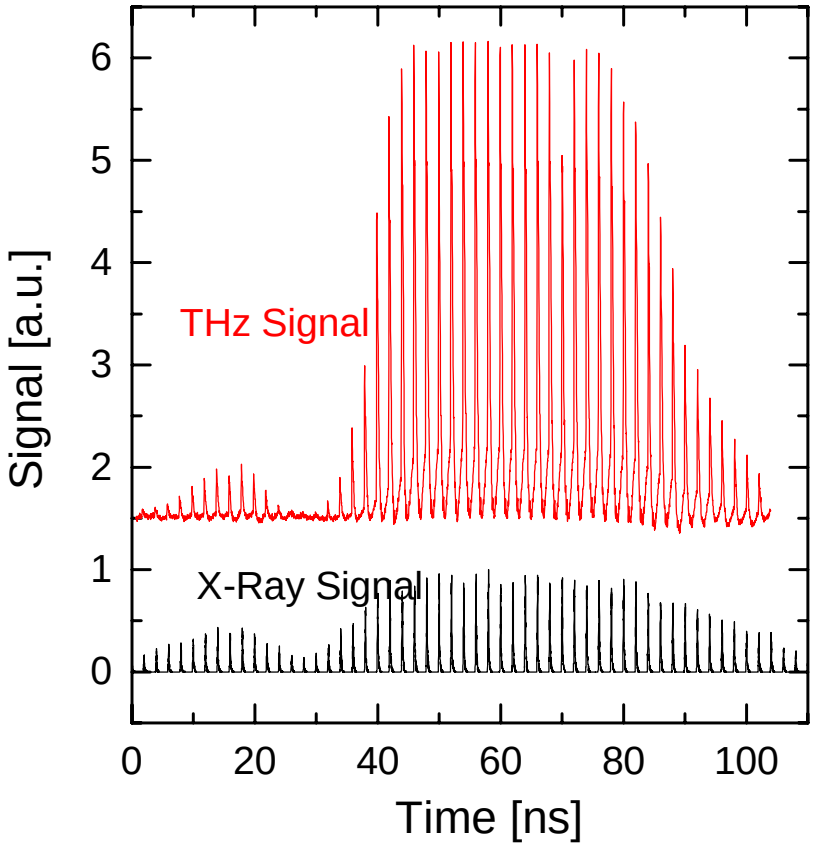

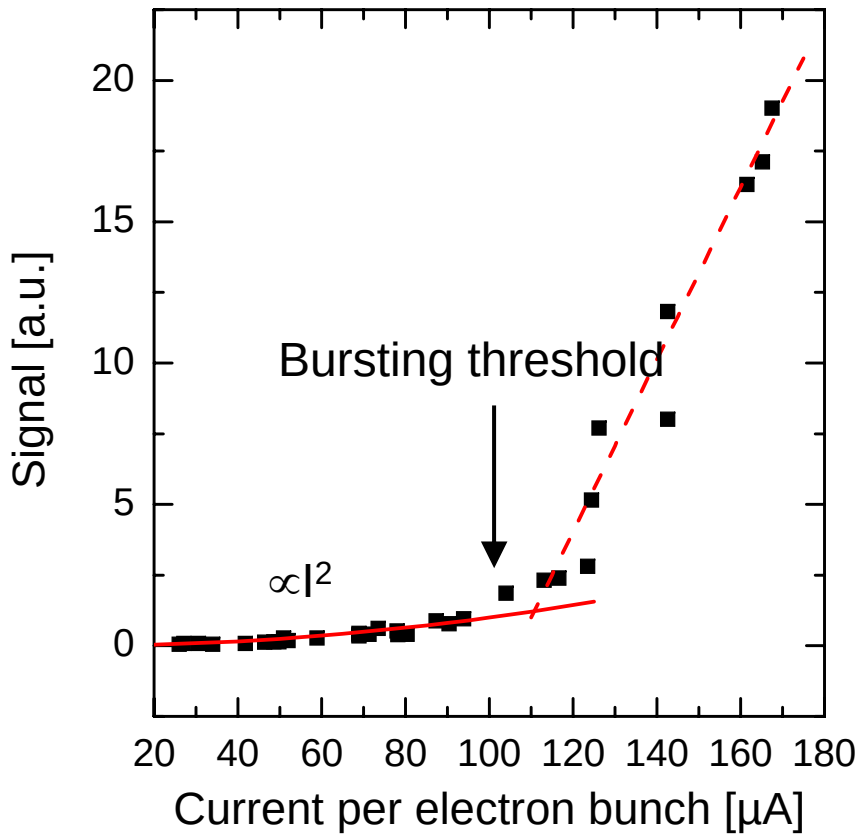

H.-W. Hübers et al., Appl. Phys. Lett. **87**, 184103 (2005)

Single Pulses Detected with a Superconducting HEB

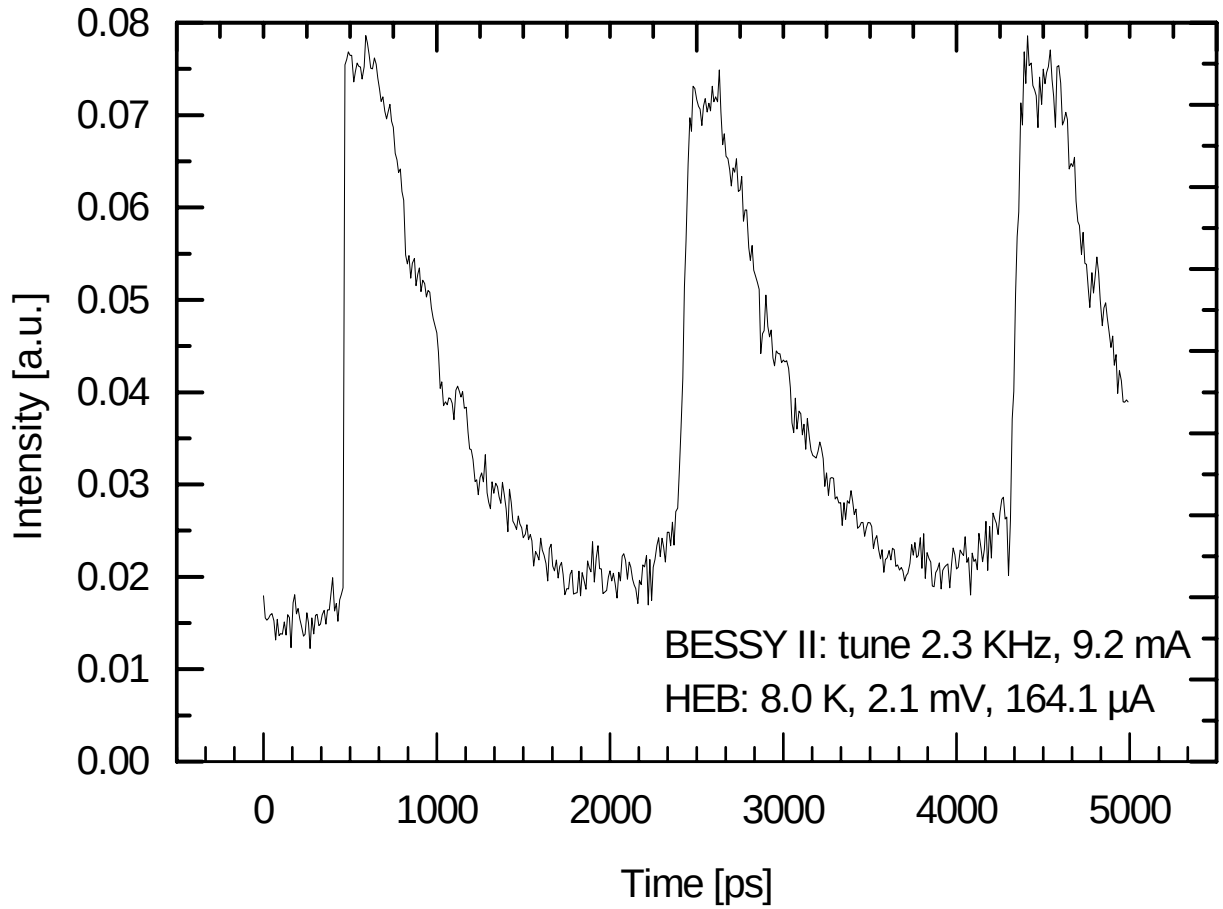

Single Pulse: Rise Time

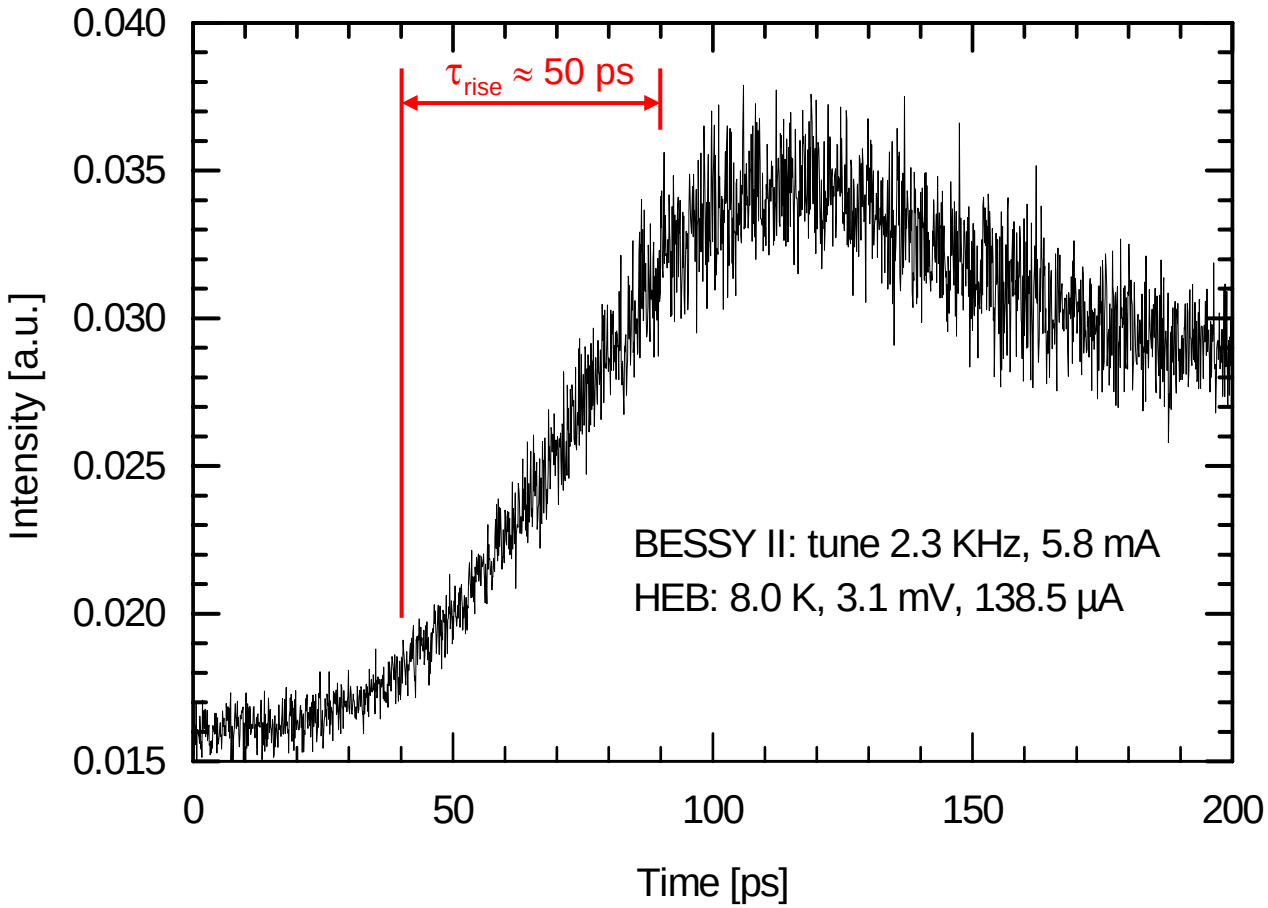

Measurement:

$\tau_{rise} \approx 50$ ps

Detector:

$\tau_{e\text{-}ph} \approx 10$ ps

$\tau_{esc} \approx 38$ ps

$\tau_{electr} \approx 35$ ps

Electron bunch:

$\tau_{FWHW} \approx 10$ ps

Single Pulse

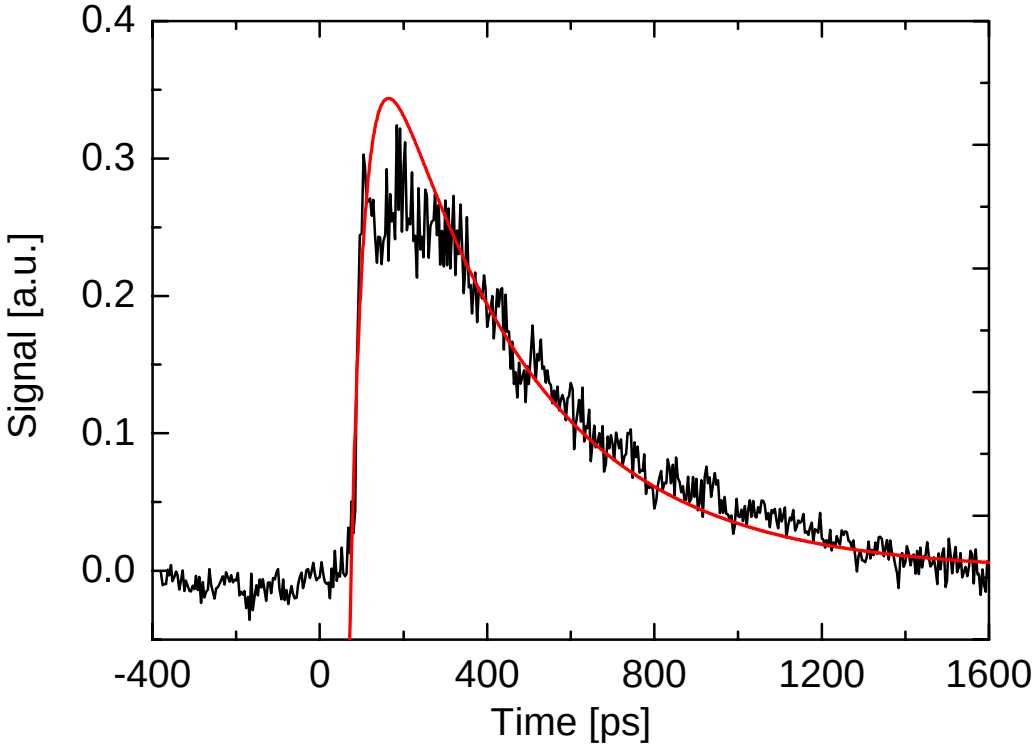

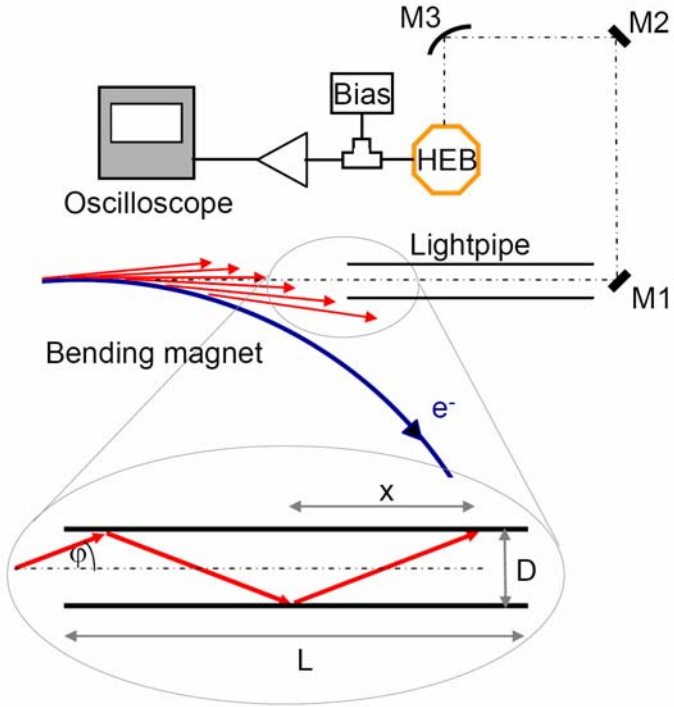

Intensity vs. time: $I(t) = I_0 R^N$

Number of reflections: $N = (L/D)\ \mathrm{tg}\varphi$

$\varphi = \mathrm{acos}(L/(L+ct))$

$R = 0.9$, $D = 170\mathrm{mm}$, $L = 9.1\mathrm{m}$

H.-W. Hübers et al., Appl. Phys. Lett. **87**, 184103 (2005)

Stable and Bursting Pulses

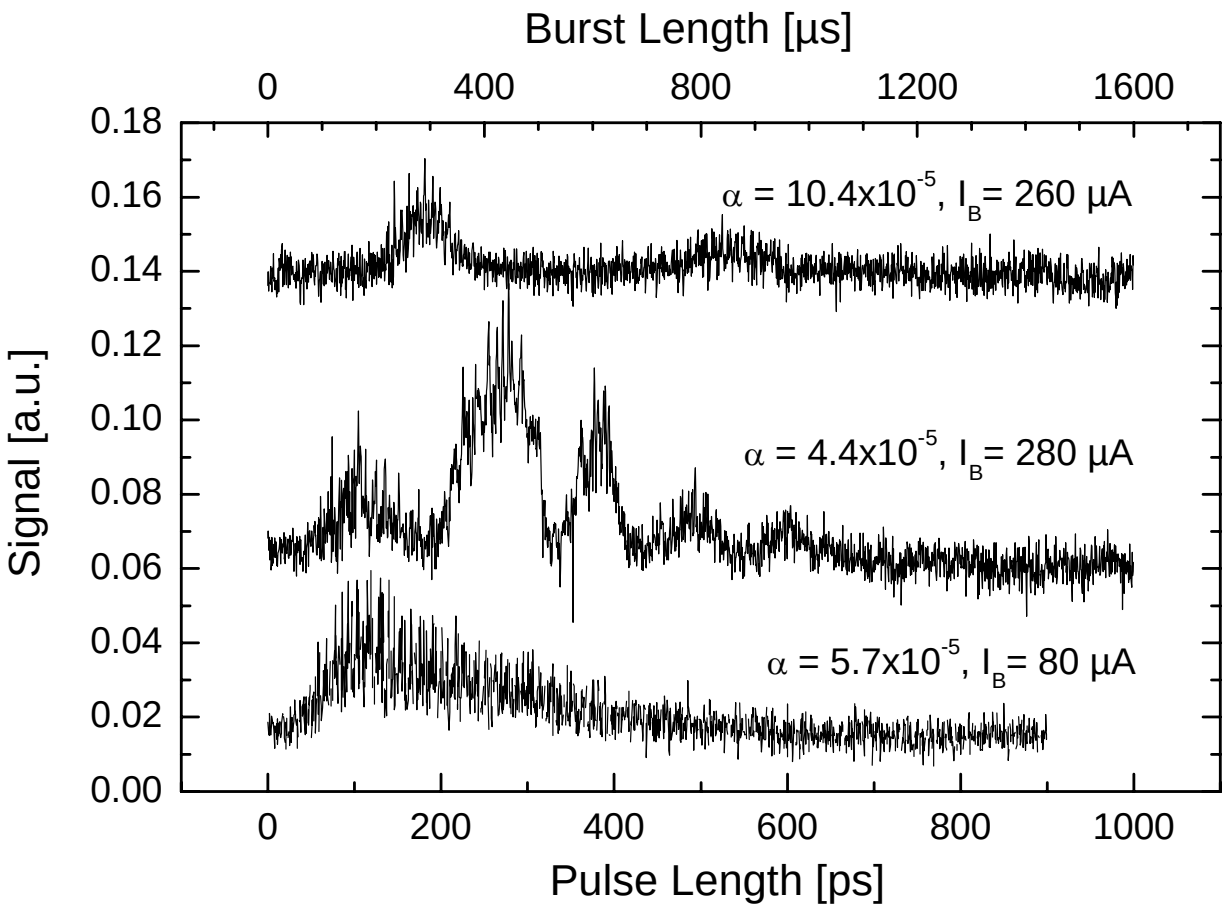

Interferograms measured with different detectors

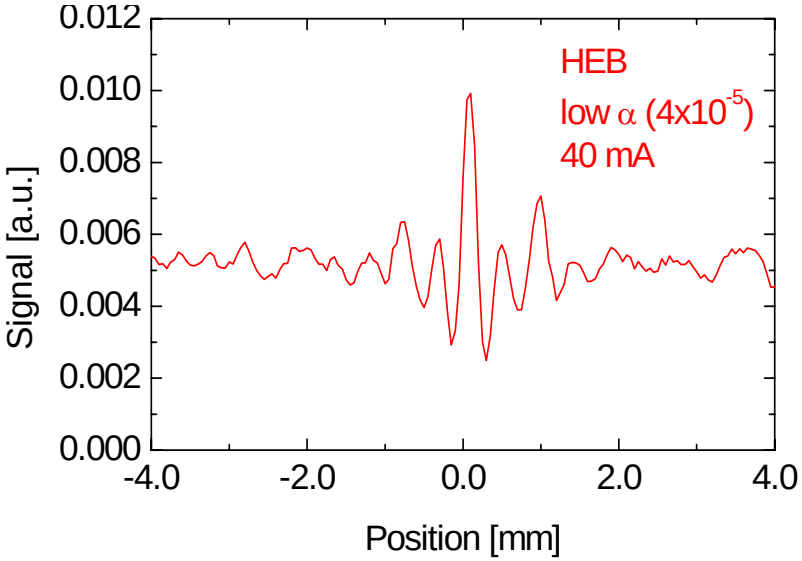

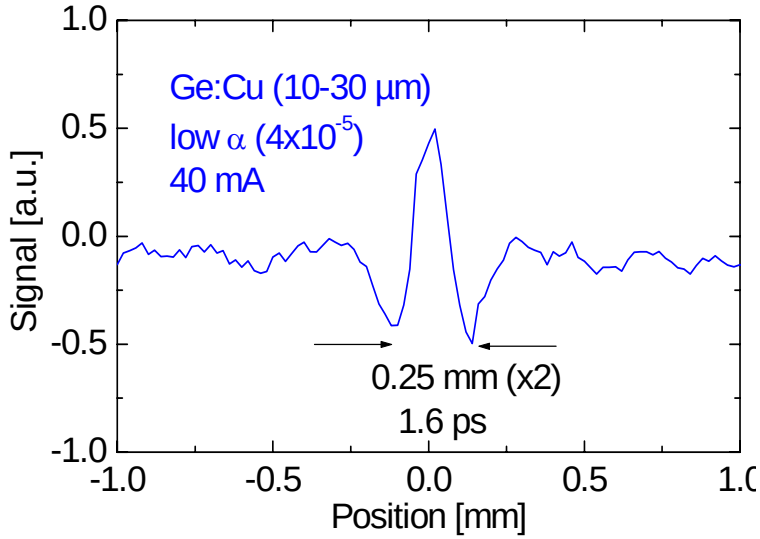

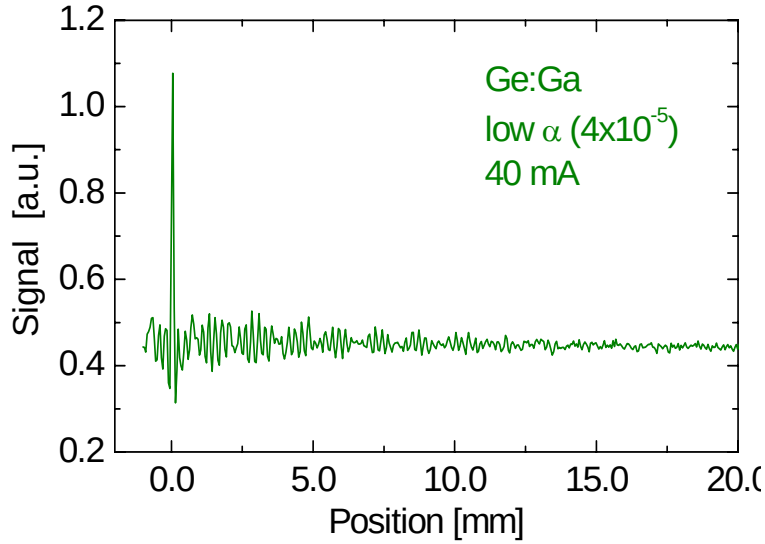

Spectrum of stable CSR

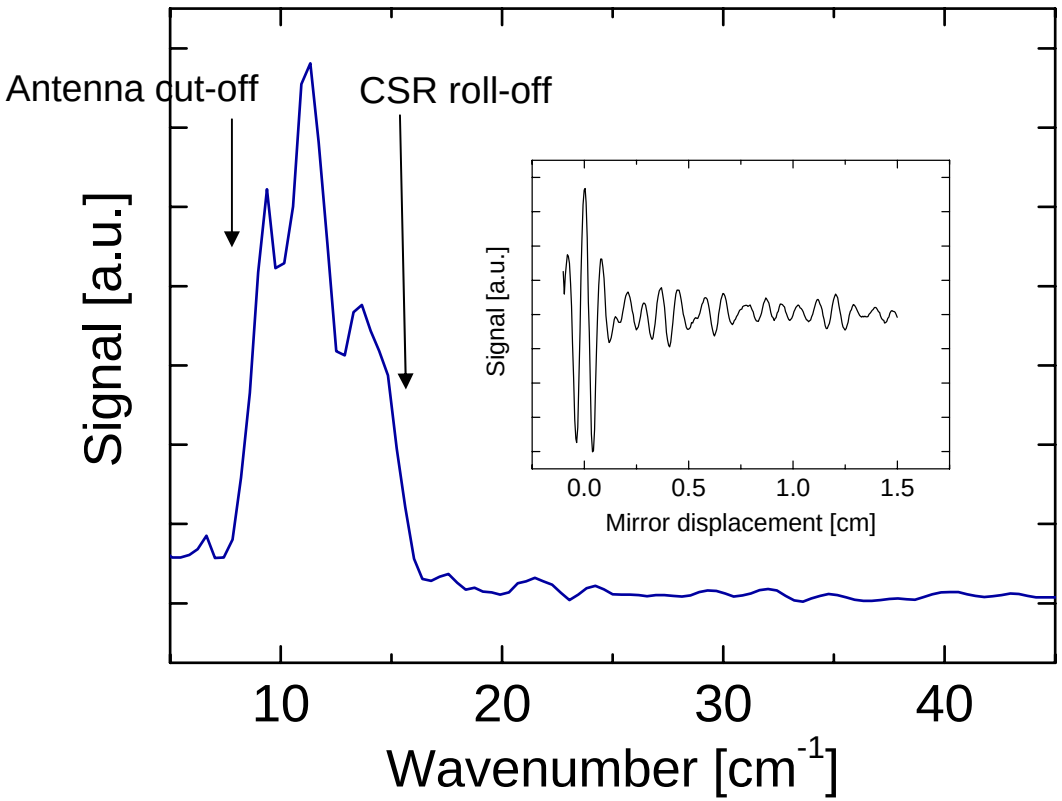

Spectrum of CSR in bursting mode

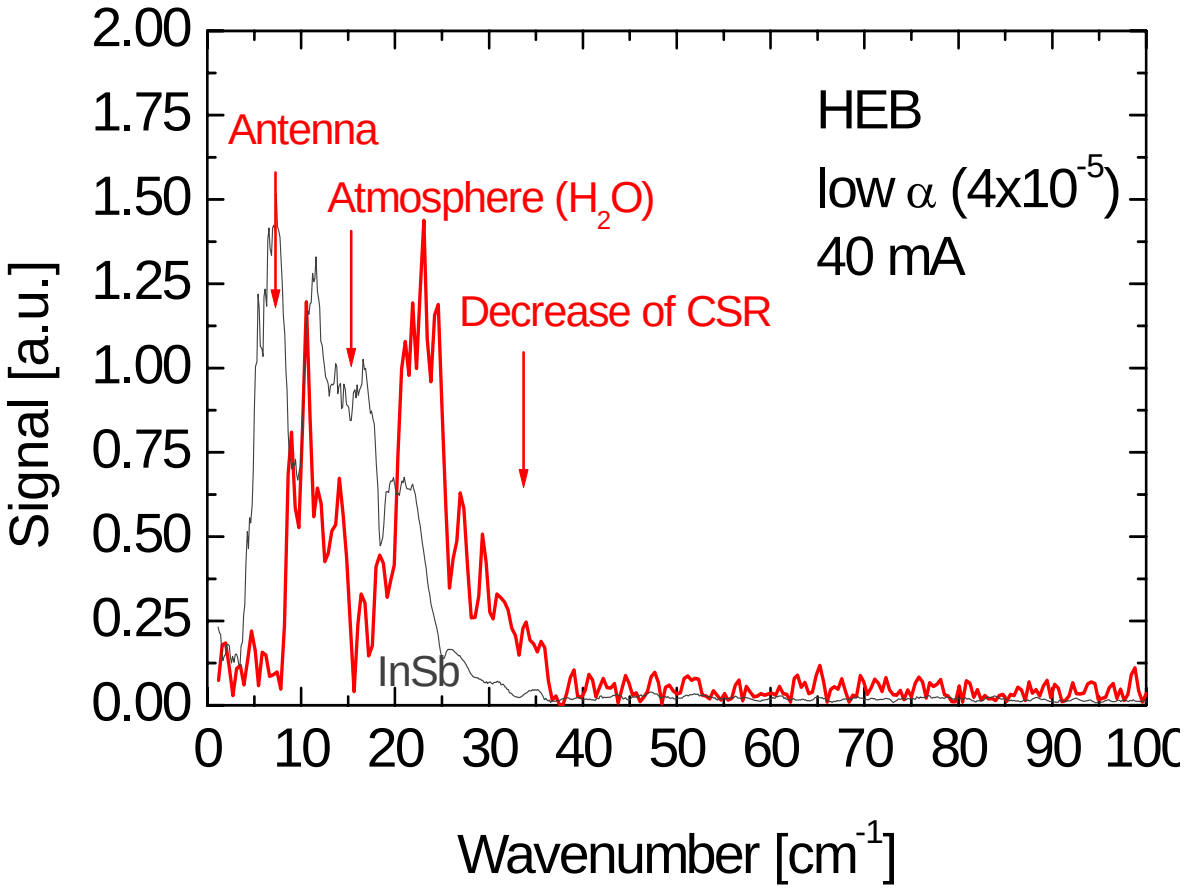

1) Synchronization of UV/Vis and THz radiation

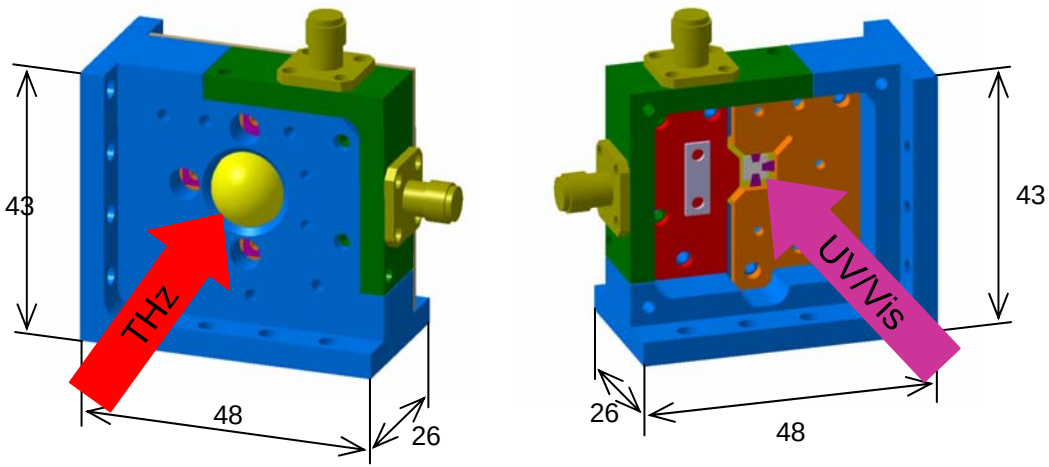

all dimensions in mm

2) Single pulse spectroscopy

Array of HEBs with resonant antennas

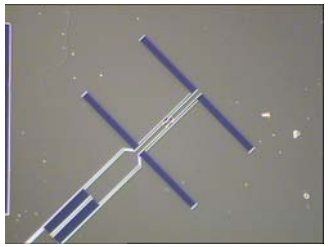

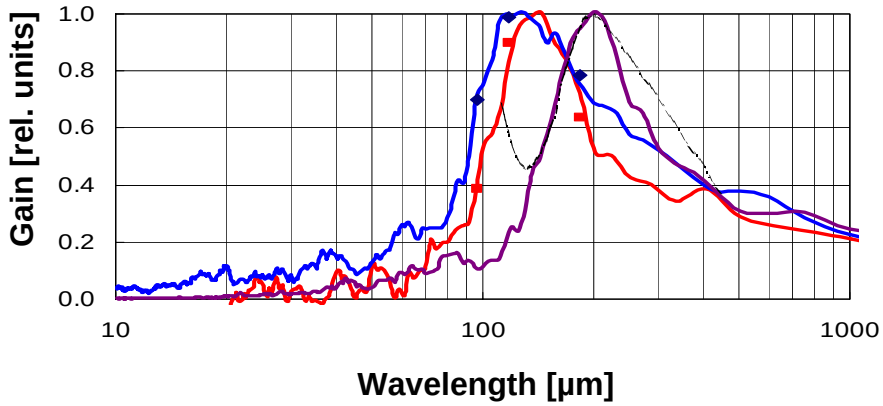

3) Faster detector with YBCO

Fast non-bolometric response (<2 ps)
but slow bolometric response (>2 ns).

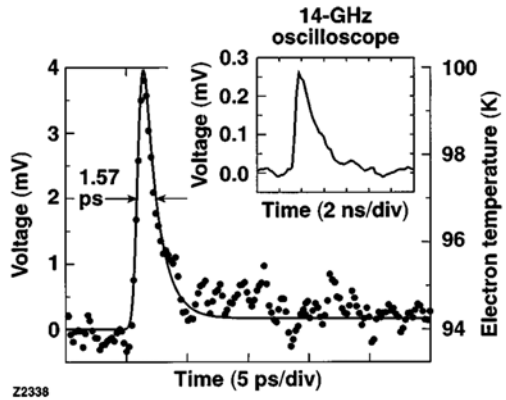

FIG. 1. Measured voltage transient (dots) and the fitted nonequilibrium electron temperature (solid line), when the bridge was biased in the resistive hot-spot state. The inset shows the bolometric part of the photoresponse, registered with the help of the 14 GHz-bandwidth oscilloscope.

M. Lindgren et al., APL **74**, 853 (1999)

4) Faster detector with electrothermal feedback

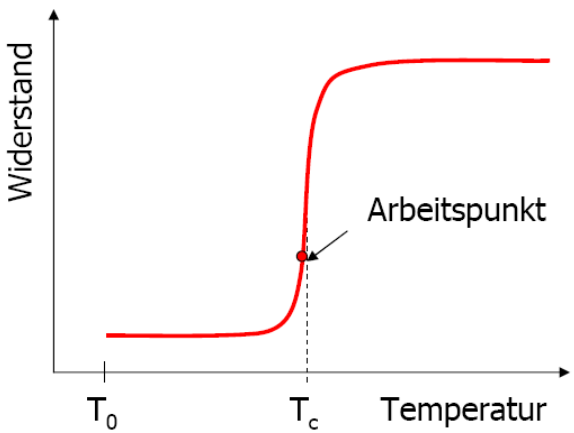

Constant voltage bias:

$T \nearrow \Rightarrow R \nearrow \Rightarrow P_{BIAS} \searrow \Rightarrow T \searrow$

$$\tau_{eff} = \frac{\tau_0}{1 + \alpha T / n}$$

~10 times faster,
but fast bias required

Thanks to

M. Greiner-Bär, S. Pavlov, H. Richter, A. D. Semenov

M. Abo-Bakr, J. Feikes, K. Holldack, U. Schade, G. Wüstefeld

Photoconductive Detectors

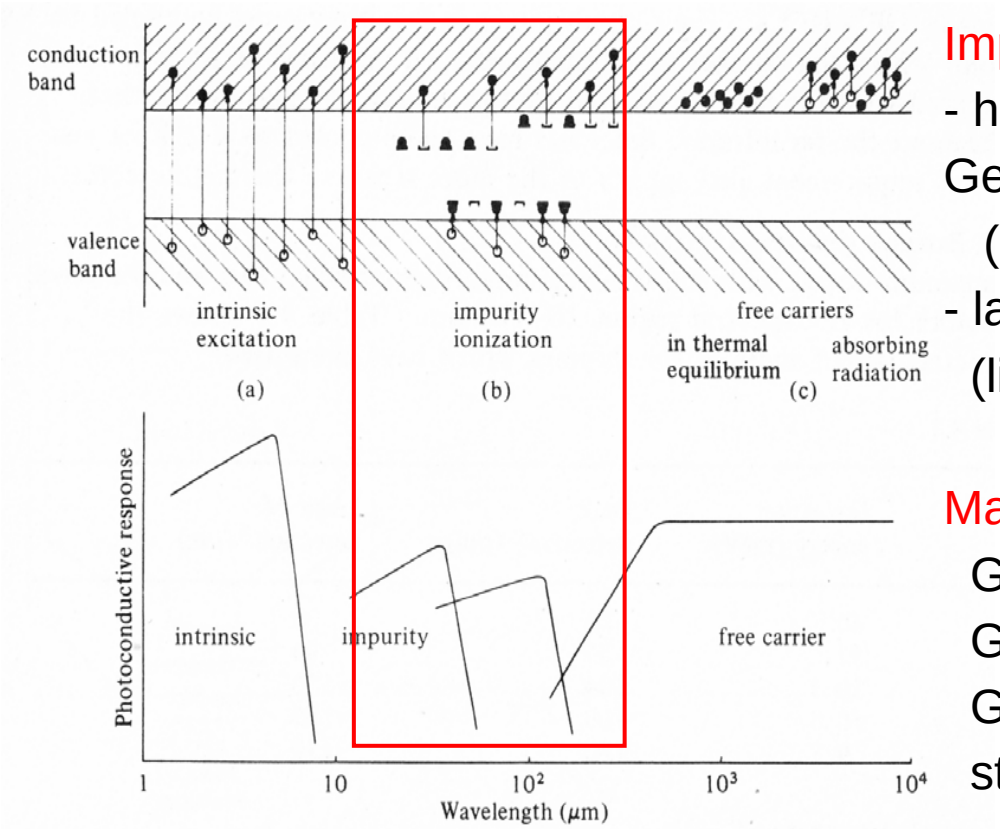

Impurity ionization

- highest sensitivity: lightly compensated p-Ge
  ($N_D \approx 10^{12}$ - $10^{13}cm^{-3}$)
- large bandwidth: compensation required
  (life time $\propto N_C^{-1}$)

Material

Ge:Cu	cut-off @ 30 µm
Ge:Be	cut-off @ 52 µm
Ge:Ga	cut-off @ 115 µm
stressed Ge:Ga	cut-off @ 210 µm

InSb-Detector: Basics

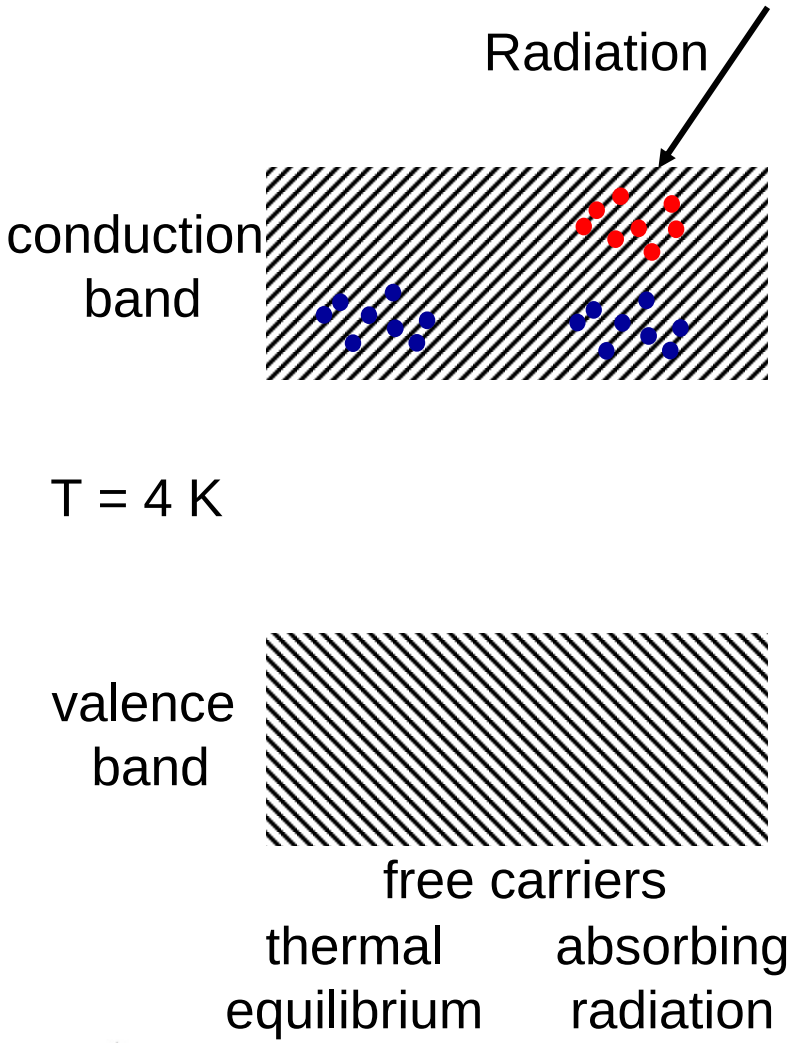

Detection mechanism:

Absorption of radiation by free electrons

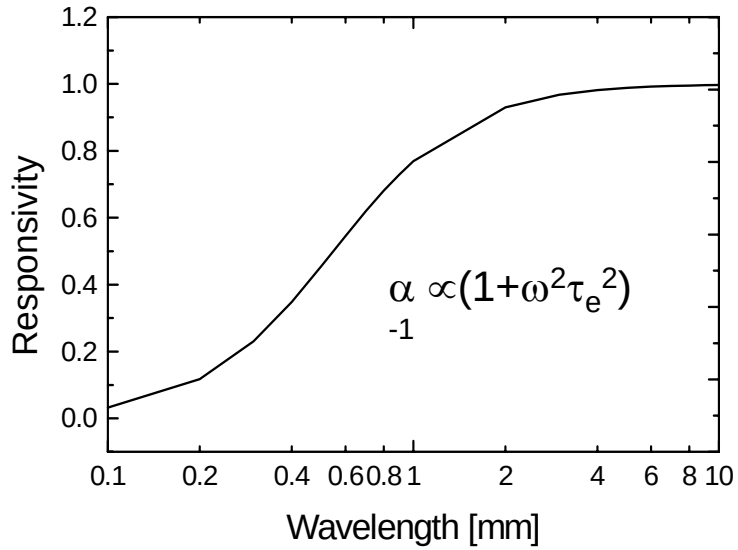

Response time: ≈ 200 nsec (≈ 1.5 MHz)

Photoionization Spectroscopy

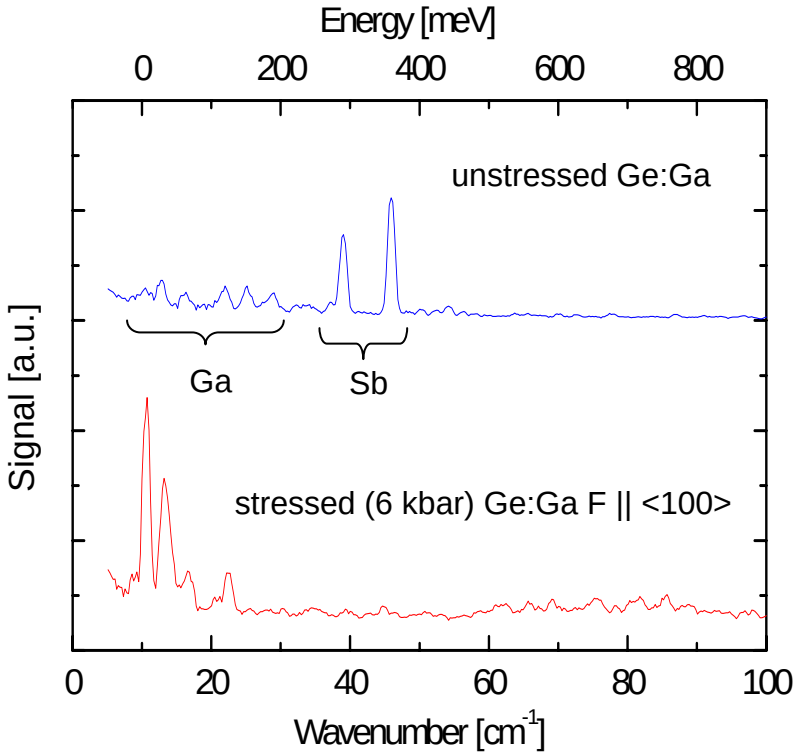

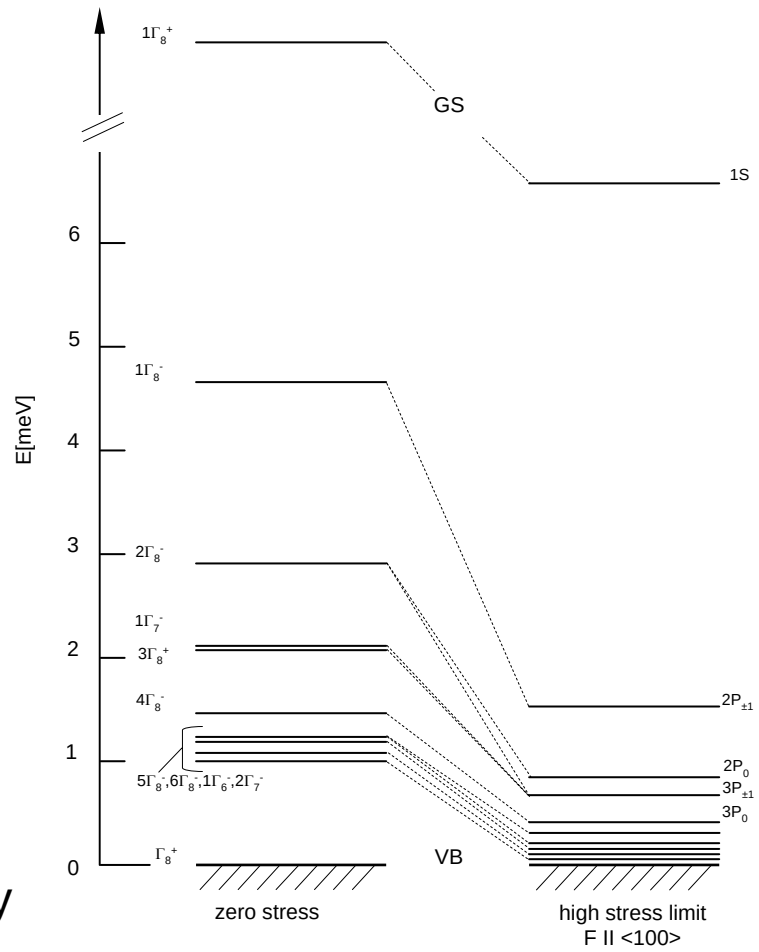

- Identification of impurity atoms
- Determination of energies
- Determination of detector responsivity